Final Report

EARLY SIGNATURES OF TWENTY FIRST CENTURY ON SNOW COVER DYNAMICS IN ZANSKAR RIVER BASIN, LADAKH

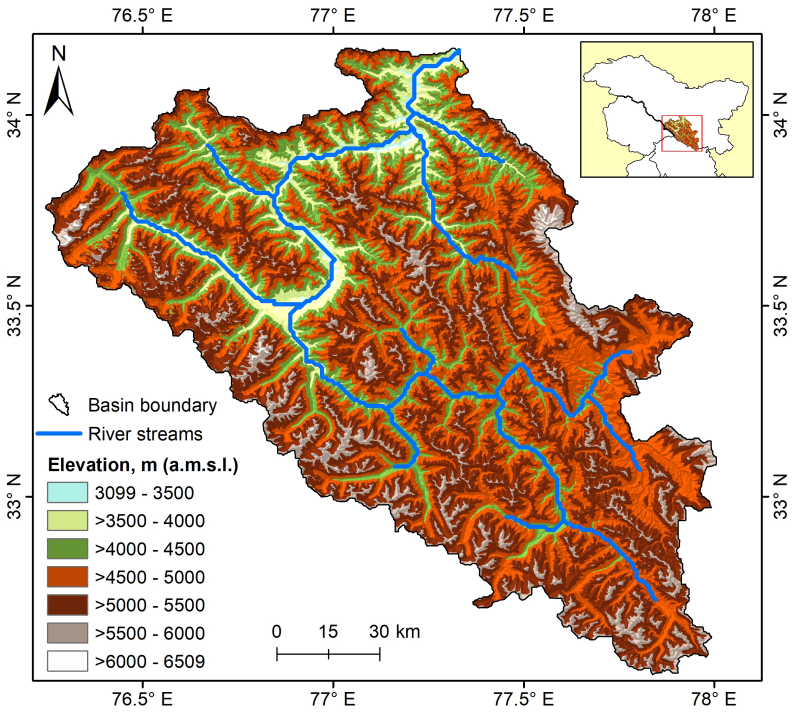

आपो हि ष्ठा मयोभुवः

Centre for Cryosphere and Climate Change Studies

National Institute of Hydrology

March 2025

Director

Dr. M.K. Goel

Head

Dr. Surjeet Singh

Study Group

Dr. D.S. Bisht (Scientist 'C')

Dr. P.G. Jose (Scientist 'E')

Abstract

The Himalayan cryosphere, encompassing vast glaciers and seasonal snow cover, is crucial for regional hydrology yet remains poorly understood, particularly in the North Western Himalayas (NWH) due to limited ground observations. Snow cover acts as a vital freshwater reservoir, regulating streamflow and groundwater recharge, with winter snowfall playing a major role in sustaining river discharge. Traditional snow cover monitoring methods are challenged by the region's rugged terrain, prompting a reliance on satellite-based remote sensing. Since 2000, MODIS sensors aboard Terra and Aqua satellites have offered high-temporal-resolution snow cover products, facilitating basin-scale snow monitoring. The Zanskar River Basin (ZRB) in Ladakh, which heavily depends on snowmelt, lacks detailed assessments of its snow cover extent (SCE) and climatic influences, impeding precise hydrological modeling and adaptation strategies.

The study employed a comprehensive methodology integrating remote sensing, geospatial analysis, and climate datasets. A total of 939 MODIS MOD10A2 eight-day composite snow products (2000–2020) at 500 m resolution were analyzed to map maximum snow extent. Elevation, slope, and aspect stratification was performed using SRTM-derived 90 m resolution digital elevation models (DEM) to explore topographic controls. For climatic trend analysis, ERA5-Land hourly temperature and precipitation data (1950–2021) at 9 km resolution were processed, with trend detection performed using the Modified Mann-Kendall test and Thiel-Sen's slope estimator across multiple overlapping 30-year climatic windows and the full 1950–2021 period. Positive Degree Days (PDD) were also calculated to capture warming impacts on the cryosphere. Results reveal strong altitudinal control over snow distribution in the ZRB, with near-perennial snow cover (>77%) persisting above 5,000 m, while below 4,000 m, snow cover variability is pronounced (0.2–95.8%). Slopes between 20° and 50° and north-facing aspects showed higher snow retention, primarily due to reduced solar exposure. Seasonally, snow cover

peaked between January and April (91–95%) and declined to a minimum in August (24%), with significant interannual variability observed, particularly during transitional months like June. Notable high snow cover years included 2009–2010, whereas low cover years, such as 2011–2012, were marked by reduced accumulation. Analysis of snowfall anomalies indicates a post-2000 increase in the frequency and severity of negative snowfall deviations, with summer (May-Oct) snowfall showing robust, statistically significant declines, suggesting a shift toward reduced snow accumulation under warming conditions.

Temperature analysis for 2000–2020 highlights the ZRB's strong thermal seasonality, with eight months averaging below freezing and an annual mean of -9.5°C. Winter (Nov-Apr) temperatures averaged -20.6°C, with January being the coldest month, while summer months (Jul-Aug) registered average temperatures just above freezing (5°C). Post-2000, the ZRB experienced accelerated warming, with 85% of years showing positive temperature anomalies relative to the 1961–1990 baseline. Statistically significant warming trends were detected across the basin, particularly in summer, emphasizing the region's vulnerability to seasonal amplification of warming. The shift in PDD post-1980 further underscores intensifying thermal forcing, with critical implications for glacier mass balance and river discharge.

Overall, this study demonstrates that the ZRB is undergoing significant cryospheric and climatic changes, driven primarily by rising temperatures and declining snowfall. The findings highlight the critical role of topographic factors in modulating snow persistence and stress the urgency of incorporating localized snow-climate interactions into regional water management and climate adaptation planning. The integration of MODIS-based snow cover monitoring with long-term reanalysis data provides a robust framework for understanding the evolving cryosphere under climate change.

Keywords: Zanskar River Basin, Snow Cover, MODIS, MOD10A2, ERA5-Land, Climate Change, Positive Degree Days, North Western Himalayas

Contents

List of Figures

List of Tables

List of Abbreviations

a.m.s.l.	Above Mean Sea Level
ECMWF	European Centre for Medium-Range Weather Forecasts
ERA5	ECMWF Reanalysis v5
GDSM	Global Digital Surface Model
ISM	Indian Summer Monsoon
MMK	Modified Mann Kendall Test
MODIS	Moderate Resolution Imaging Spectroradiometer
NWH	North Western Himalayas
PDD	Positive Degree Days
SCE	Snow Cover Extent
SCA	Snow Covered Area
w.e.	Water Equivalent
WMO	World Meteorological Organization
ZRB	Zanskar River Basin

Chapter 1

Introduction

1.1 Background

The Himalayan region is characterized by extensive glaciation and ephemeral snow cover, which constitute vital components of the cryosphere. These elements exert a profound influence on hydrological systems in mountainous areas, yet their precise effects within the Himalayas are not fully elucidated, largely owing to a paucity of observational records. As a key terrestrial variable in global hydrological and energy dynamics, snow cover modulates radiative feedback mechanisms at various spatial scales while functioning as an essential freshwater reserve within the hydrological system (Jain et al., 2008). Regionally, snow cover plays an indispensable role in sustaining water supply, regulating streamflow, and facilitating groundwater replenishment, particularly in mid- to high-latitude zones. In the North Western Himalayas (NWH), substantial snowfall accumulation occurs due to frigid winter conditions and elevated topography, with subsequent snow and glacial melt constituting a major contribution to river discharge. Hydrological modeling efforts frequently integrate snow-covered area (SCA) metrics with hydro-meteorological parameters to estimate snowmelt-derived runoff (Aggarwal et al., 2014). Nevertheless, conventional techniques for assessing seasonal snow cover encounter significant limitations, including sparse instrumentation, logisti-

cal constraints in winter accessibility, complex terrain, and the isolation of these regions. In response, satellite remote sensing has proven to be an invaluable approach for assessing snow cover, glacial boundaries, and high-altitude water bodies, providing enhanced temporal and spatial precision (Aggarwal et al., 2014). Since the year 2000, the Terra (EOS AM) and Aqua (EOS PM) satellites, carrying the Moderate-Resolution Imaging Spectroradiometer (MODIS), have been supplying daily, 8-day, and 16-day snow cover area (SCA) products. Notably, the MOD10A2 and MYD10A2 datasets—providing 8-day maximum snow cover extent at a 500-meter resolution (Hall et al., 2001)—have been widely employed in snow cover assessments (Shukla et al., 2017; Snehmani et al., 2016). The generation of these products relies on a snow mapping algorithm that incorporates the Normalized Difference Snow Index (NDSI) alongside supplementary threshold-based assessments (Hall et al., 1995).

Over the past four decades, the Himalayan region has witnessed accelerated glacial retreat, a phenomenon strongly linked to global warming (Maurer et al., 2019). Projected increases in temperature are anticipated to further alter snow cover patterns, thereby influencing the hydrological regimes of snowmelt-dependent river systems. Reanalysis datasets, such as ERA5-Land, which offer extensive climatological records, serve as valuable tools for examining the interplay between climatic variability and cryospheric processes. For example, Dharpure et al. (2020) leveraged ERA5-Land reanalysis data to evaluate climate-induced shifts in snow cover dynamics within the Chenab River basin.

Despite these advancements, there remains a critical gap in localized studies examining snow cover extent in conjunction with regional climatic trends. Existing research predominantly adopts a macro-scale approach, covering either the entire northwestern Himalayas or the broader Himalayan arc, thereby neglecting finer-scale regional variations. Furthermore, the availability of satellite-derived snow cover data since 2000, combined with high-resolution reanalysis products, presents an unprecedented opportunity to assess climate change impacts on snow cover dynamics. Such analyses are imperative for formulating adaptive strategies to mitigate the consequences of climatic shifts in the Himalayan cryosphere.

1.2 Problem Definition

The Himalayan cryosphere, particularly in the high-altitude Ladakh region, serves as a critical freshwater reservoir, with snow and glacier melt contributing significantly to river discharge and groundwater recharge in the Zanskar River basin. However, the spatiotemporal dynamics of snow cover extent (SCE) and its sensitivity to climate change remain insufficiently characterized due to the region's complex topography, extreme climatic conditions, and lack of in-situ monitoring infrastructure. Conventional ground-based snow surveys and sparse meteorological stations face severe limitations in this rugged, remote terrain, resulting in fragmented and discontinuous datasets that impede robust hydrological assessments.

While satellite remote sensing—particularly MODIS (Moderate Resolution Imaging Spectroradiometer) 8-day snow cover products (e.g., MOD10A2/ MYD10A2) — has enabled systematic SCE monitoring since 2000, prior studies have predominantly focused on macro-scale analyses (e.g., entire North-West Himalayas or pan-Himalayan assessments). These broad-scale approaches often overlook micro-scale heterogeneities introduced by elevation-dependent temperature gradients, slope-aspect-driven solar radiation variability, and localized precipitation patterns, all of which govern snow accumulation and ablation processes. Consequently, the absence of high-resolution, basin-specific SCE analyses limits the accuracy of snowmelt runoff models and climate adaptation strategies in the Zanskar basin.

Furthermore, the accelerating impacts of climate change—evidenced by rising temperatures and shifting precipitation regimes—are disproportionately affecting high-mountain cryospheric systems. Yet, quantitative assessments of long-term SCE trends (2001–2020) and their climatic drivers (e.g., temperature anomalies, reanalysis-derived snowfall variability) remain sparse for the Zanskar basin. This knowledge gap undermines predictive capacity for future water availability, as snowmelt timing and magnitude directly influence river discharge regimes, irrigation planning, and ecosystem stability in this arid, snow-dependent region.

1.3 Objectives of the study

Given the critical role of snow cover in regulating water resources and regional hydrology and hydrological response, a mechanistic understanding of snow-climate-hydrology interactions in the Zanskar River basin (Ladakh, northwestern Himalayas) is essenatial. Despite advancements in remote sensing and climate reanalysis data, key knowledge gaps persist regarding (i) the topographic controls on snow distribution, (ii) seasonal and interannual snow cover variability, and (iii) long-term cryospheric responses to climate change. Addressing these gaps is essential for improving hydrological predictions and climate adaptation strategies in this data-scarce, high-altitude region.

To systematically investigate these aspects, the study seeks to answer the following research questions:

- How does snow cover extent (SCE) vary across different elevation bands, slope gradients, and aspect classes in the Zanskar basin, and what are the dominant topographic controls on its spatial distribution?
- What are the intra-annual patterns of SCE, i.e., how it evolves during different months of the year?
- How the climate change (temperature and precipitation anomalies) have been experienced by the region in the retrospective period which can have the implication on cryospheric stability in the region?

By addressing these questions, the study can enhance the understanding of snow-climate-hydrology interactions in the Zanskar basin, contributing to improved water resource management in the northwestern Himalayas. Therefore following three key objectives formulated to investigate climate-cryosphere linkage in the Zanskar basin using open source remote sensing and reanalysis data:

1. To analyze the spatial distribution of snow cover extent in Zanskar River basin with respect to elevation, slope, and aspect.

2. To analyze the seasonal variability in snow cover extent in Zanskar River basin .

3. To investigate the impact of climate change on snow cover extent during 2001-2020.

1.4 Chapterization

This report is structured and organized into five chapters as follows,

Chapter-1 presents an overview of the study, problem statement and specifies the major objectives. It also summaries the organization of the report.

Chapter-2 provides the description of study area i.e., Zanskar River basin (ZRB) in brief. It also discusses the dataset used in the study in brief.

Chapter-3 describes the methodology used in the study and present the brief details of concepts employed for analyzing the climate and remote sensing data to address to decipher the climate-cryosphere linkage.

Chapter-4 presents the results of analysis pertaining to snow cover extent variability across space and time. It also discusses the climate change over the retrospective period which has direct implication on changing cryosphereic response of the basin.

Chapter-5 summarizes the report in brief and presents the key conclusion drawn from the study. It also presents the limitation of the present work and scope for future study.

Chapter 2

Study Area and Data Used

2.1 Description of Study area

The Ladakh Himalayas constitute a high-altitude cold desert, situated within the orogenic belt between the Greater Himalayan ranges to the south and the Karakoram ranges to the north. This geomorphologically dynamic region is predominantly shaped by fluvial processes associated with the Indus River system, among which the Zanskar River serves as a significant northeast-flowing tributary within the upper Indus River basin. The Zanskar River basin (ZRB), encompassing an area of approximately 15,000 km^2 (Figure 2.1), is strategically positioned in the Western Himalayan region (Ladakh) and is demarcated by distinct hydrological boundaries: the Suru basin to the west, the Spiti Valley (an extension of the upper Sutlej basin) to the southeast, and the Lahul district to the south. ZRB's hydrological system is primarily sustained by two major tributaries: (i) the Doda River, originating from Pensi La Pass (4,400 m a.m.s.l.), and the Tsarap Lingti Chu, a high-altitude glacial stream. These tributaries converge at Padam, forming the mainstem Zanskar River, which ultimately joins the Indus River at Nimu (Chahal et al., 2019).

The Zanskar valley is geologically defined by two distinct units: the Great Himalayan Range to the southwest and the Zanskar Range to the northeast. A

2.1. Description of Study area

glacier inventory based on Survey of India topographical maps identifies ≈268 glaciers within the basin, distributed between elevations of 3,600 m and 6,478 m a.m.s.l. Of these, 131 glaciers are located in the Higher Himalaya, while 137 glaciers reside in the Zanskar Mountains (Sharma & Phartiyal, 2020).

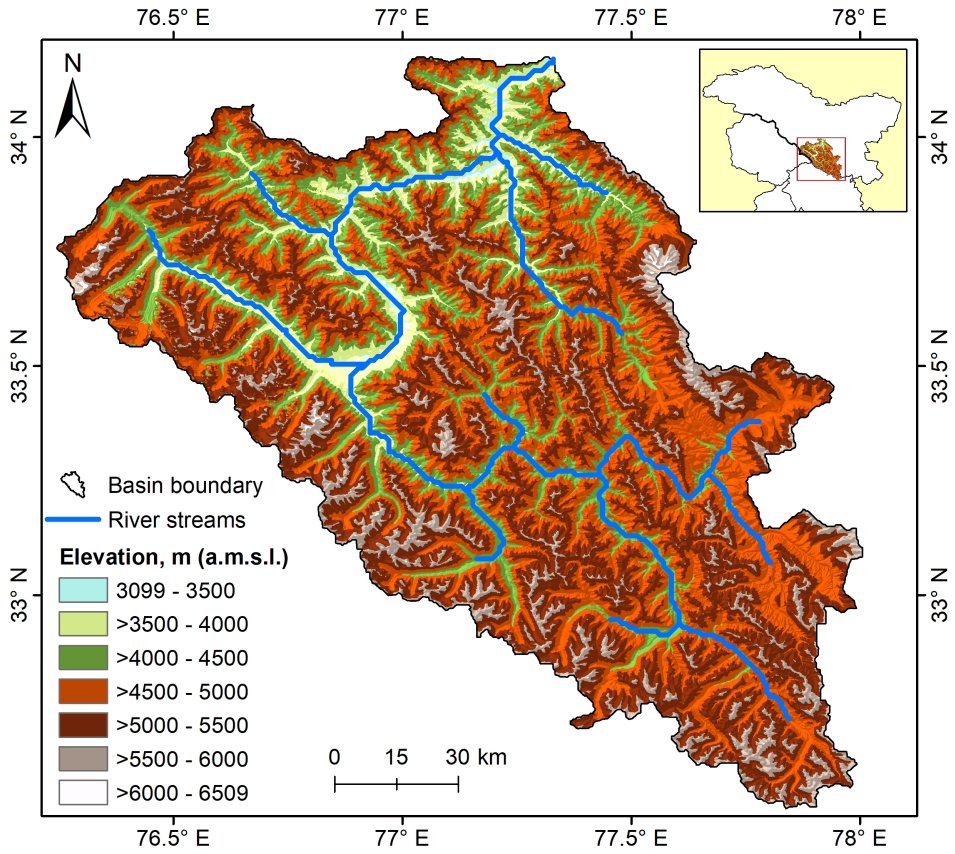

Figure 2.1: Topographic map of study area, river streams and catchment delineated using SRTM Digital Elevation Model

Climatically, the region exhibits a pronounced bimodal influence. The southern part of the catchment, dominated by the Higher Himalayan Crystallines (HHC), receives significant precipitation from the Indian Summer Monsoon (ISM). In contrast, the northern sector, comprising the Ladakh Batholith, lies in the rain shadow of the Greater Himalayas, resulting in hyperarid conditions (Chahal et al., 2019). The moisture availability in ZRB is regulated by a complex interplay of ISM and western disturbances (Ali et al., 2020). Thus the precipitation patterns

in the ZRB exhibit a dual-phase regime:

- Summer rainfall (July–September), driven by ISM incursions, though spatially restricted to lower elevations.
- Winter snowfall (December–March), associated with mid-latitude westerlies, which contributes significantly to glacial and snowpack accumulation.

The ZRB is typified by an extreme continental climate, marked by strong seasonal thermal variability. Winter temperatures frequently plummet to $-14°C$, while summer maxima can reach $24.7°C$, reflecting the region's pronounced diurnal and seasonal temperature fluctuations (Taylor & Mitchell, 2000). Vegetation cover in ZRB is highly restricted, confined predominantly to riparian corridors and alluvial terraces, owing to the prevailing moisture deficit and low soil organic content.

2.2 Description of Data Used

In this study, remote sensing data derived from MODIS imagery were utilized to analyze the spatial and temporal variability of snow cover extent, while ERA5-Land reanalysis data were employed to examine the long-term climatology of the basin. For topographic classification of the ZRB the SRTM 90m Digital Elevation Model (DEM) was utilized. A brief description of these datasets is provided below.

2.2.1 MODIS remote sensing data

MOD10A2 is a snow cover dataset derived from the Moderate Resolution Imaging Spectroradiometer (MODIS) onboard the Terra satellite. This dataset provides the maximum snow cover extent observed over an eight-day period at a spatial resolution of 500 meters. The eight-day compositing period aligns with the ground track repeat cycle of the Terra and Aqua satellite platforms, ensuring consistent

temporal coverage. Within each composite period, snow cover is represented in two ways: as the maximum snow extent observed on any single day and as a chronological sequence of daily observations. The eight-day periods are calculated starting from the first day of the year and may extend into the following year. While the product is designed to include up to eight days of input data, the actual number of days may vary due to factors such as cloud cover or data acquisition issues. This dataset has been widely used for monitoring snow cover dynamics, hydrological modeling, and climate studies due to its high temporal and spatial resolution.

2.2.2 SRTM 90m Digital Elevation Model

The Shuttle Radar Topography Mission (SRTM) 90 m Digital Elevation Model (DEM) is a freely accessible globally recognized elevation dataset designed to support geospatial research and sustainable development initiatives. Processed to address data voids and enhance usability, it provides seamless topographic coverage for over 80% of the Earth's surface. The dataset features a spatial resolution of 3 arc-seconds (approximately 90 meters at the equator). To ensure data continuity, voids in the original SRTM DEM were filled using interpolation algorithms and supplementary elevation data by the providers. Distributed by the United States Geological Survey (USGS), it remains a cornerstone for hydrological modeling, terrain analysis, climate studies, and infrastructure planning. Its void-filled processing and global reach make it particularly valuable for regions lacking high-resolution elevation data, advancing cross-disciplinary research and informed decision-making aligned with sustainable development goals.

2.2.3 ERA5-Land data

ERA5-Land is a high-resolution ($0.1^\circ \times 0.1^\circ$) reanalysis dataset that offers a consistent and comprehensive view of land surface variables over multiple decades. Produced by replaying the land component of the ECMWF ERA5 climate reanalysis, it integrates model data with global observations using physical laws

to generate a globally complete and temporally consistent dataset. The dataset spans several decades, enabling the analysis of long-term climatic trends and historical land surface conditions.The atmospheric forcing for ERA5-Land is derived from ERA5 atmospheric variables, including air temperature, humidity, and pressure, which are corrected for altitude differences between the forcing grid and the higher-resolution ERA5-Land grid using a 'lapse rate correction.' While observations are not directly assimilated into ERA5-Land, they indirectly influence the dataset through the atmospheric forcing, ensuring a realistic representation of land surface processes. The dataset's high temporal and spatial resolution, combined with its extensive temporal coverage and fixed grid structure, makes it a powerful tool for researchers, decision-makers, and businesses seeking accurate and reliable information on land surface states and dynamics. For this study, three ERA5-land datasets (Table 2.1) were obtained for the period spanning 1950-2021.

Table 2.1 Description of ERA5-Land hourly data used

S. No.	Data	Description
1	2m Temperature (K)	Temperature of air at 2m above the surface of land, sea or in-land waters.
2	Snowfall (m.w.e.)	Accumulated total snow that has fallen to the Earth's surface. It consists of snow due to the large-scale atmospheric flow (horizontal scales greater than around a few hundred metres) and convection where smaller scale areas (around 5km to a few hundred kilometres) of warm air rise. If snow has melted during the period over which this variable was accumulated, then it will be higher than the snow depth. This variable is the total amount of water accumulated from the beginning of the forecast time to the end of the forecast step.

Continued on next page

Table 2.1 – *Continued from previous page*

S. No.	Data	Description
3	Total Precipitation (m)	Accumulated liquid and frozen water, including rain and snow, that falls to the Earth's surface. It is the sum of large-scale precipitation (that precipitation which is generated by large-scale weather patterns, such as troughs and cold fronts) and convective precipitation (generated by convection which occurs when air at lower levels in the atmosphere is warmer and less dense than the air above, so it rises). Precipitation variables do not include fog, dew or the precipitation that evaporates in the atmosphere before it lands at the surface of the Earth. This variable is accumulated from the beginning of the forecast time to the end of the forecast step.

Chapter 3

Methodology

The present study adopts a structured and interdisciplinary methodological framework to investigate the complex dynamics of snow cover variability and its climatic drivers within the Zanskar River basin (ZRB). This comprehensive approach synergistically integrates remote sensing techniques, high-resolution climatological reanalysis data, and statistical methods to ensure robust, spatially explicit, and temporally resolved insights into cryospheric processes and their responses to climate variability. This approach was followed to address key scientific questions regarding snow cover distribution patterns, long-term climatological trends, and their interrelationships. In subsequent sections detail about snow cover and climate data analysis is elaborated.

3.1 Snow cover analysis

The methodology employed in this study to analyze the snow cover dynamics of the ZRB is both comprehensive and systematic, leveraging advanced remote sensing and geospatial techniques to ensure robust and reliable results. A total of 939 MODIS images from the TERRA satellite, specifically the MOD10A2 product—an eight-day composite land surface reflectance dataset—were acquired for the period spanning 2000 to 2020. This product is particularly valuable as it

provides the maximum extent of snow cover observed over an eight-day period at a spatial resolution of 500 meters, capturing the days on which snow was present within this timeframe. The maximum snow extent is defined as areas where snow was detected on at least one day during the eight-day interval, offering a detailed temporal perspective on snow cover variability.

To facilitate a nuanced analysis of snow cover distribution, the ZRB was stratified into distinct zones based on elevation, slope, and aspect, which are critical topographic factors influencing snow accumulation and melt processes. Prior to this stratification, the SRTM 90 m DEM was utilized to generate detailed elevation, slope, and aspect maps of the study area. These maps served as the foundational datasets for delineating the basin into 03 elevation bands (Figure 3.1), six slope bands (Figure 3.2) and eight aspect bands (Figure 3.3) as detailed in Table 3.1.

Table 3.1 Elevation, Slope, and Aspect Classification

Elevation Class	Elevation Range (m, a.m.s.l.)	Slope Class	Slope Range (Degree)	Aspect Class	Aspect Orientation
Entire	> 3099	Zone 1	$0 - 10$	Zone 1	North
Zone 1	$3099 - 4000$	Zone 2	$10 - 20$	Zone 2	North-East
Zone 2	$4000 - 5000$	Zone 3	$20 - 30$	Zone 3	East
Zone 3	> 5000	Zone 4	$30 - 40$	Zone 4	South-East
		Zone 5	$40 - 50$	Zone 5	South
		Zone 6	> 50	Zone 6	South-West
				Zone 7	West
				Zone 8	North-West

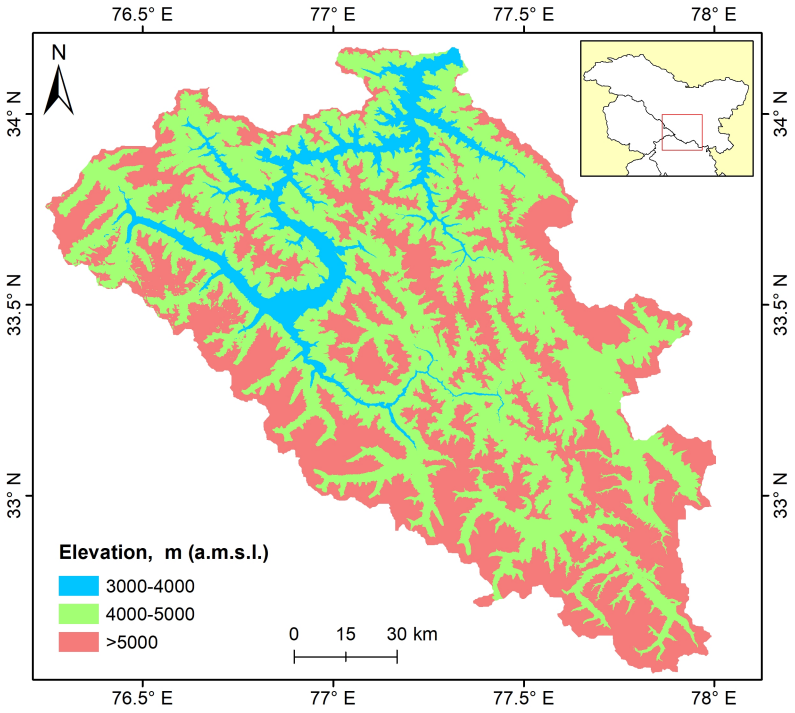

Figure 3.1: Categorized elevation zones in ZRB

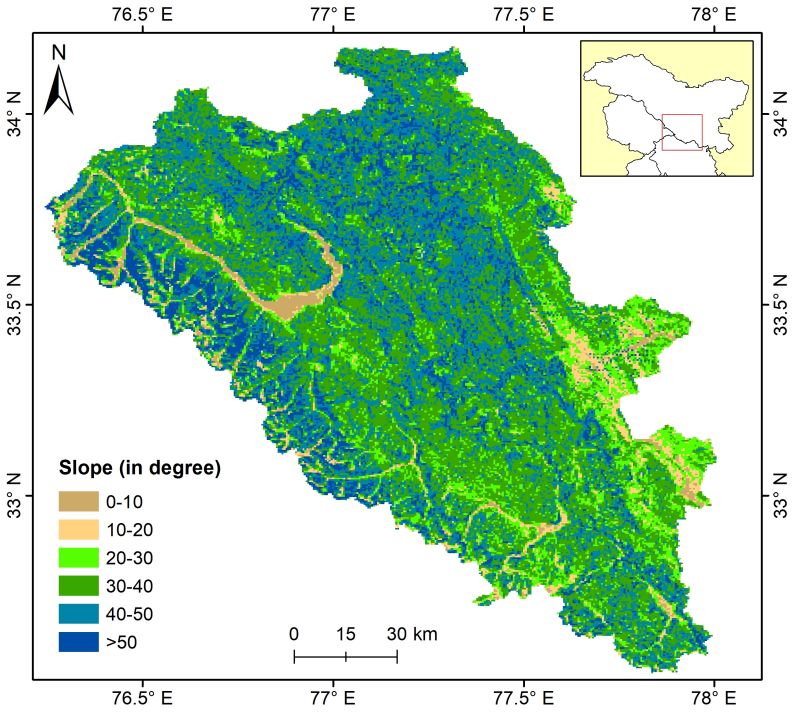

Figure 3.2: Categorized slope zones in ZRB

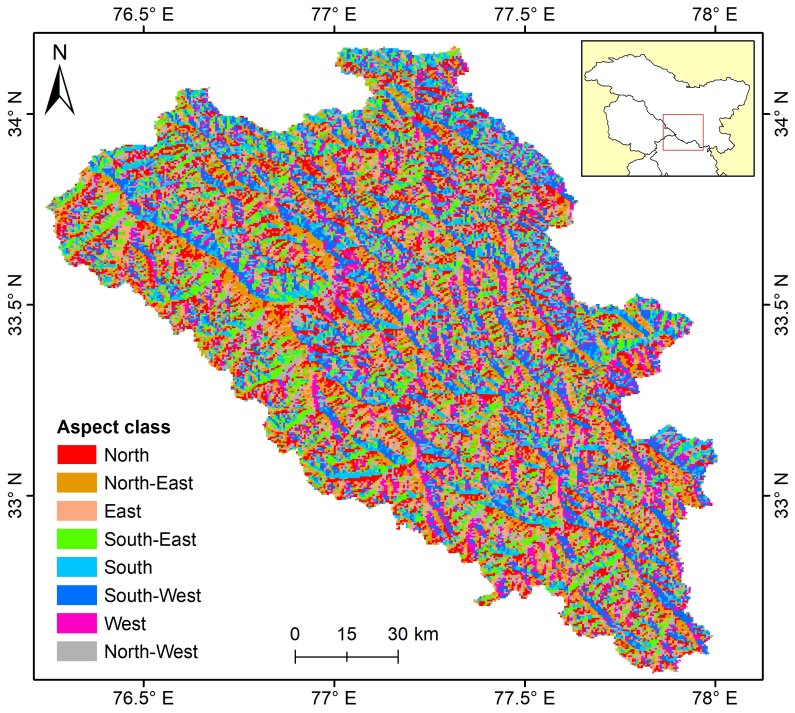

Figure 3.3: Categorized aspect zones in ZRB

3.2 Climatological analysis

ERA5-Land data, widely used for its high temporal and spatial consistency, ensures robust insights into the interplay between climatic variables and snow cover dynamics, thereby enhancing the scientific understanding of cryospheric responses to global warming. To investigate the influence of global warming, driven by climate change, on snow cover dynamics, ERA5-Land hourly datasets for total precipitation and air temperature were acquired for the length of 72-year from 1950 to 2021. These datasets, available at a spatial resolution of 9 $km \times 9$ km, provide a seamless and comprehensive spatiotemporal record for analysis.

To extract meaningful insights from climatological data, the time series were systematically analyzed for trends. The Modified Mann-Kendall test, a robust non-parametric method for trend detection, was employed to assess

trends in snowfall and temperature. These analyses were conducted across multiple 30-year climatic windows—1951–1980, 1961–1990, 1971–2000, 1981–2010, and 1991–2020—along with an evaluation of the long-term trend spanning the entire period of record (1950–2020). The magnitude of statistically significant trends was quantified using Thiel-Sen's slope estimator. All trend analyses were performed at a 5% significance level employing the readily available statistical functions developed by Hussain & Mahmud (2019). A comprehensive description of the Modified Mann-Kendall test and Thiel-Sen's slope estimation methodology is provided in Bisht et al. (2018). Furthermore, the anomaly in the snowfall and temperature were also studied with respect to the reference period of 1961-1990 to understand the shift in these climatological variables with respect to long term climate change as per the recommendation made by WMO (2017).

To understand the influence of rising temperatures on accelerated snowmelt in the Zanskar River Basin (ZRB), Positive Degree Days (PDD) metric was employed. PDD refer to the cumulative sum of daily temperatures above 0 °C over a given period, typically used in glaciology and hydrology to estimate snow and ice melt. The PDD approach assumes that melting is directly proportional to the amount of time and the extent to which temperatures remain above freezing. This index is widely utilized in degree-day melt models, which provide a simple yet effective way to quantify snow and glacier melt, particularly in regions where detailed energy balance data are unavailable. The significance of PDD lies in its ability to correlate temperature variations with melt rates, offering insights into seasonal and long-term changes in cryospheric processes. Increased PDD values indicate enhanced melting, often associated with climate warming and altered hydrological regimes. This has critical implications for water resource management, flood risks, and glacier mass balance studies, making PDD an essential parameter in climate change assessments and hydrological modeling. The anomalies in the PDD across the basin were studied to understand how the PDDs have changed over the period.

Chapter 4

Results and Discussion

This study systematically analyzed snow cover dynamics and climatic drivers in the ZRB using multi-source remote sensing data and reanalysis products. MODIS snow cover products (2000-2020) were processed with strict cloud-cover filtering (<15%) to examine spatial patterns across elevation zones (3,099-4,000 m, 4,000-5,000 m, >5,000 m), slope categories (0-10° to >50°), and eight cardinal aspects. ERA5-Land data (1950-2020) were employed to investigate temperature trends, snowfall variability, and Positive Degree Day (PDD) anomalies, with statistical significance assessed using Modified Mann-Kendall tests and Thiel-Sen's slope estimator. The analysis quantified seasonal snow cover persistence, identified temporal trends in climatic variables, and evaluated their interrelationships through gridded spatial analysis and regional averaging.

4.1 Spatial Distribution of Snow Cover

The multi-criteria stratification of the basin based on altitude, slope and aspects allow for a granular examination of snow cover dynamics across diverse topographic conditions. The variation in snow cover extent was quantified with respect to maximum, minimum, and average snow cover values over the 20-year study period, with results systematically analysed for each elevation band, slope band,

and aspect. This approach not only enhances the understanding of spatial and temporal snow cover patterns but also provides critical insights into the interplay between topography and cryospheric processes, which is essential for hydrological modeling, climate change impact assessments, and water resource management in high-altitude regions.

4.1.1 Snow cover extent vs elevation

A comprehensive analysis of snow cover distribution across different elevation zones in ZRB stratified by altitude bands is presented in Table 4.1. The zones are categorized as Entire Region (>3099 m), Zone 1 (3,099–4,000 m), Zone 2 (4,000–5,000 m), and Zone 3 (>5,000 m), each characterized by its specific areal extent and corresponding snow cover dynamics.

Table 4.1 Snow cover characteristics by elevation zone

Elevation class	Elevation range (m, a.m.s.l.)	Area (km^2)	Pixel count	% annual areal snow cover		
				Max	Min	Average
Entire	$> 3,099$	14,809	69,011	98.3	17.0	63.6
Zone 1	3,099−4,000	1,143	5,328	95.8	0.2	38.2
Zone 2	4,000−5,000	7,452	34,725	98.9	4.8	55.9
Zone 3	$> 5,000$	6,214	28,958	99.9	33.4	77.9

The areal extent ranges from 1,143 km^2 in Zone 1 to 7,452 km^2 and 6,214 km^2 in Zones 2 and 3, respectively. The total area analyzed across all elevation bands encompasses 14,809 km^2, represented by 69,011 pixels in the MOD10A2 imagery. The analysis reveals a distinct altitudinal gradient in snow cover persistence, with higher elevations exhibiting consistently greater snow cover on an average throughout the year for the period of 2000-2020. Specifically:

- The Entire Region exhibits a wide range of annual snow cover, with values ranging from a minimum of 17% to a maximum of 98.3%, and an average of 63.6%.

- Zone 1 (3,0994,000 m), which constitutes the lowest elevation band analyzed, shows the lowest snow persistence, with an average annual snow cover of 38.2% and a substantial variability between 0.2% minimum and 95.8% maximum, reflecting significant seasonal fluctuations and possibly higher interannual variability.
- Zone 2 (4,000–5,000 m) demonstrates moderate-to-high snow cover presence, with a mean annual snow cover of 55.9%, minimum of 4.8%, and a maximum of 98.9%, indicating a transitional zone where both seasonal snowmelt and persistent snow coexist.
- Zone 3 (>5,000 m), comprising the highest elevation band, exhibits near-perennial snow cover with a mean of 77.9%, and very high persistence (maximum 99.9%, minimum 33.4%), indicative of cold climatic conditions and reduced seasonal melt.

This elevational insight in snow cover dynamics emphasizes the strong influence of altitude on snow accumulation and persistence. Such patterns are critical for hydrological modeling, climate impact assessments, and water resource planning in ZRB.

4.1.2 Snow cover extent vs slope

An analysis of the spatial distribution and persistence of snow cover across varying slope gradients within the ZRB is presented in Table 4.2. The slope is stratified into six discrete classes, ranging from gentle slopes (0–10°) in Zone 1 to steep slopes (>50°) in Zone 6, allowing for an assessment of how terrain steepness influences snow cover characteristics.

The areal extent varies considerably across slope classes, with the smallest area occurring in Zone 1 (297 km^2) and the largest in Zone 4 (5,748 km^2), reflecting the natural predominance of mid-range slopes within the terrain. The total analyzed area spans 14,859 km^2, represented by 69,250 pixels in the MOD10A2 imagery.

Table 4.2 Snow cover characteristics by slope zone

Slope class	Slope range (degree)	Area (km^2)	Pixel count	% annual areal snow cover		
				Max	Min	Average
Zone 1	0−10	297	1,385	99.5	23.1	54.7
Zone 2	10−20	646	3,014	99.0	22.9	58.8
Zone 3	20−30	1,889	8,803	98.6	14.3	60.6
Zone 4	30−40	5,748	26,787	98.4	13.0	63.9
Zone 5	40−50	4,655	21,693	98.1	16.7	63.8
Zone 6	> 50	1,624	7,568	98.7	30.8	68.6

Snow cover shows notable variation across slope bands, though the maximum annual snow cover remains consistently high across all classes (>98%), indicating widespread seasonal snow accumulation regardless of slope steepness. However, average and minimum snow cover percentages reveal more nuanced trends:

- Zone 1 (0–10°), representing flat to gently sloping terrain, shows a moderate mean snow cover of 54.7% with a minimum of 23.1%, possibly due to increased solar radiation absorption and accumulation of debris or vegetation that may limit snow retention.

- Zone 2 (10–20°) displays a slightly higher average snow cover of 58.8%, indicating improved snow retention possibly due to reduced melt rates on moderately inclined surfaces.

- Zone 3 (20–30°) and Zone 4 (30–40°) show further increases in average snow cover (60.6% and 63.9%, respectively), with Zone 4 also covering the largest area. This suggests that these intermediate slope ranges provide optimal conditions for snow accumulation and preservation, balancing gravitational shedding and insolation effects.

- Zone 5 (40–50°) maintains a high average snow cover of 63.8%, though slightly lower than the steepest class.
- Zone 6 (>50°) exhibits the highest average snow cover (68.6%) and a notably high minimum of 30.8%, despite the steep terrain. This counterintuitive pattern could be attributed to reduced direct solar exposure, particularly on north-facing slopes, or wind-driven deposition in concave topographies.

The analysis indicates that while maximum snow cover is uniformly high, average snow cover, interestingly, decreases with slope, reflecting complex interactions between slope geometry, aspect, solar radiation, and wind redistribution. These findings underscore the importance of incorporating slope information into snow hydrology models and climate impact assessments in ZRB.

4.1.3 Snow cover extent vs aspect

Aspect, representing the directional orientation of slopes, is a crucial topographic factor influencing the amount and duration of solar radiation received at the surface. This, in turn, significantly affects snow accumulation and melt patterns, leading to distinct variations in snow cover persistence across aspect bands. The analysis divides the study area into eight primary aspect classes—North, North-East, East, South-East, South, South-West, West, and North-West—each with its corresponding areal extent, pixel representation, and statistical range of annual snow cover percentages. An in-depth analysis of snow cover dynamics across different terrain aspect classes is presented in Table 4.3.

- The North facing slopes (Zone 1), encompassing an area of 2,190 km^2 and represented by 10,204 pixels, exhibit the highest snow retention among all aspect classes. The percent annual snow cover in this zone ranges from a minimum of 23.2% to a maximum of 98.9%, with an average value of 68.2%, indicating strong snow persistence due to limited direct solar radiation.
- The North-East facing slopes (Zone 2) cover an area of 2,170 km^2 (10,112 pixels) and display a similar snow cover profile, with minimum, maximum,

Table 4.3 Snow cover characteristics by aspect zone

Aspect class	Aspect range (directional)	Area (km^2)	Pixel count	% annual areal snow cover		
				Max	Min	Average
Zone 1	North	2,190	10,204	98.9	23.2	68.2
Zone 2	North−East	2,170	10,112	98.9	17.5	64.9
Zone 3	East	1,652	7,702	99.0	17.7	66.1
Zone 4	South−East	1,792	8,349	98.3	17.6	63.8
Zone 5	South	1,823	8,727	97.2	15.0	58.5
Zone 6	South−West	1,975	9,202	97.5	12.3	57.9
Zone 7	West	1,518	7,074	98.3	12.7	62.2
Zone 8	North−West	1,691	7,878	98.9	17.8	66.7

and average values of 17.5%, 98.9%, and 64.9%, respectively. The slightly lower average compared to the northern slopes reflects early morning solar exposure, which accelerates melt to a small extent but still allows for high snow retention.

- The East facing slopes (Zone 3), covering 1,652 km^2 with 7,702 pixels, receive morning sunlight and show a high degree of snow presence, with a minimum of 17.7%, a maximum of 99.0%, and an average of 66.1%. This average, slightly higher than that of the North-East zone, suggests that while early sun exposure initiates melt, the snow retention is still relatively strong due to typically cooler morning temperatures.

- The South-East aspect (Zone 4) spans an area of 1,792 km^2 (8,349 pixels) and records annual snow cover percentages between 17.6% and 98.3%, with an average of 63.8%. The reduction in average snow cover compared to eastern aspects points to stronger insolation during the late morning to midday period, enhancing ablation processes.

- The South facing slopes (Zone 5), which are directly exposed to the sun throughout the day, display the lowest snow persistence. With an areal extent of 1,823 km^2 and 8,727 pixels, the annual snow cover ranges from a minimum of just 15.0% to a maximum of 97.2%, and an average of 58.5%.

This low average value is indicative of high melt rates and reduced snow duration due to prolonged and intense solar exposure.

- The South-West facing slopes (Zone 6), which experience strong afternoon sun, cover an area of 1,975 km^2 (9,202 pixels) and show the lowest minimum snow cover among all zones at 12.3%. Although the maximum value reaches 97.5%, the average snow cover remains low at 57.9%, reflecting enhanced melting conditions during the warmer part of the day.

- The West facing slopes (Zone 7), with an extent of 1,518 km^2 and 7,074 pixels, receive dominant afternoon solar radiation and exhibit moderate snow cover conditions. The percent annual snow cover in this zone varies from 12.7% to 98.3%, averaging 62.2%, suggesting relatively balanced accumulation and melt dynamics.

- The North-West facing slopes (Zone 8), covering 1,691 km^2 and represented by 7,878 pixels, demonstrate snow cover statistics comparable to other northern orientations, with a minimum of 17.8%, a maximum of 98.9%, and an average of 66.7%. These values confirm that northwestern slopes, like their northern counterparts, maintain high snow persistence due to reduced exposure to intense solar radiation, especially during critical melting periods.

The snow cover analysis across aspect zones highlights the strong influence of terrain orientation on snowpack behavior. Northern aspects consistently retain more snow throughout the year due to reduced insolation, whereas southern and southwestern slopes exhibit significantly lower snow persistence, driven by higher solar energy input and consequent ablation. These spatial variations are critical for understanding hydrological processes, planning water resources, and modeling climate impacts in snow-dominated regions of ZRB.

4.2 Temporal Analysis of Snow Cover Extent

The snow cover variability was also examined on monthly basis across the basin during 2000-2020. For this a total of 931 MODIS images were analysed. Monthwise variabiltty of snow cover is presented in Figure 4.1. It is to be noted that, the monthwise snow cover variability was presented for the days for which cloud cover is found to be less than 15%. Cloud cover extent for respective snow cover variabilities presented in Figure 4.1 is illustrated in Figure 4.2. For a cloud cover of 15% or more over the basin the snow cover analysis was excluded to avoid potential errors due to data gap.

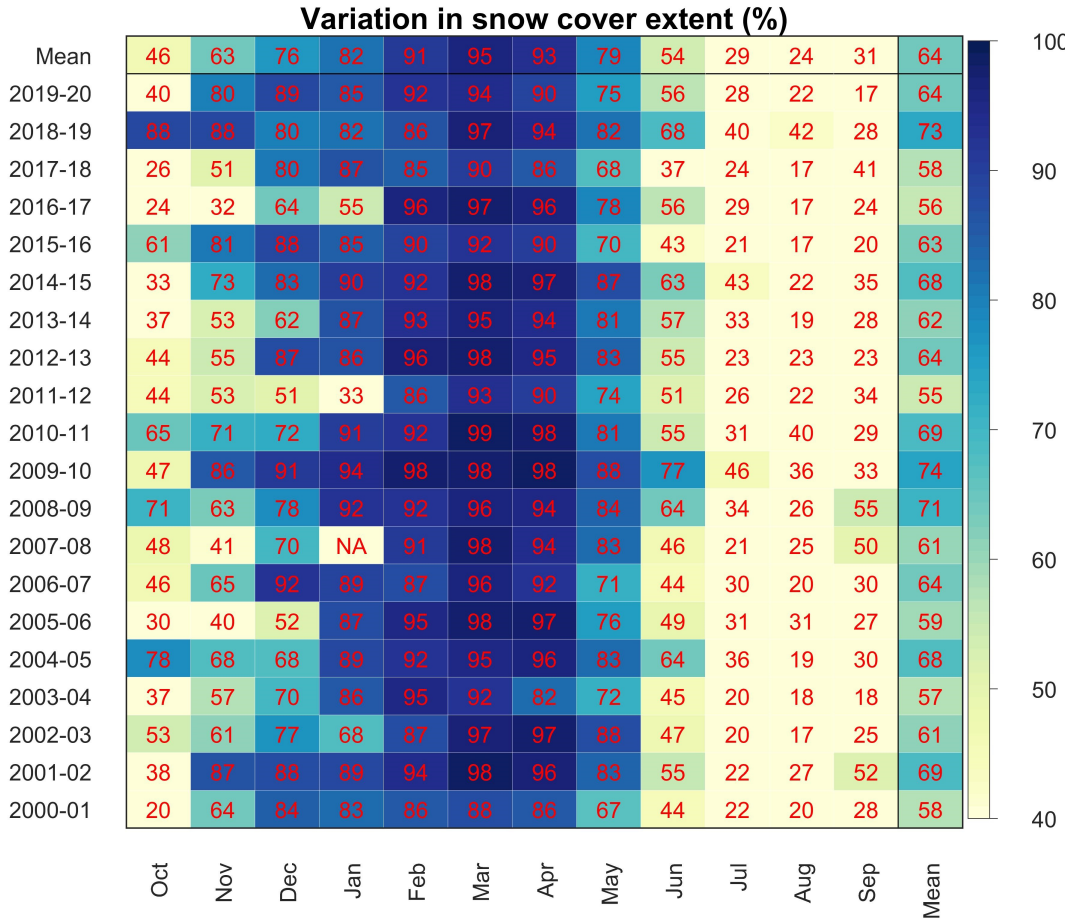

Figure 4.1: Variation in month-wise average snow cover extent (in % of total basin area) during 2000-2020

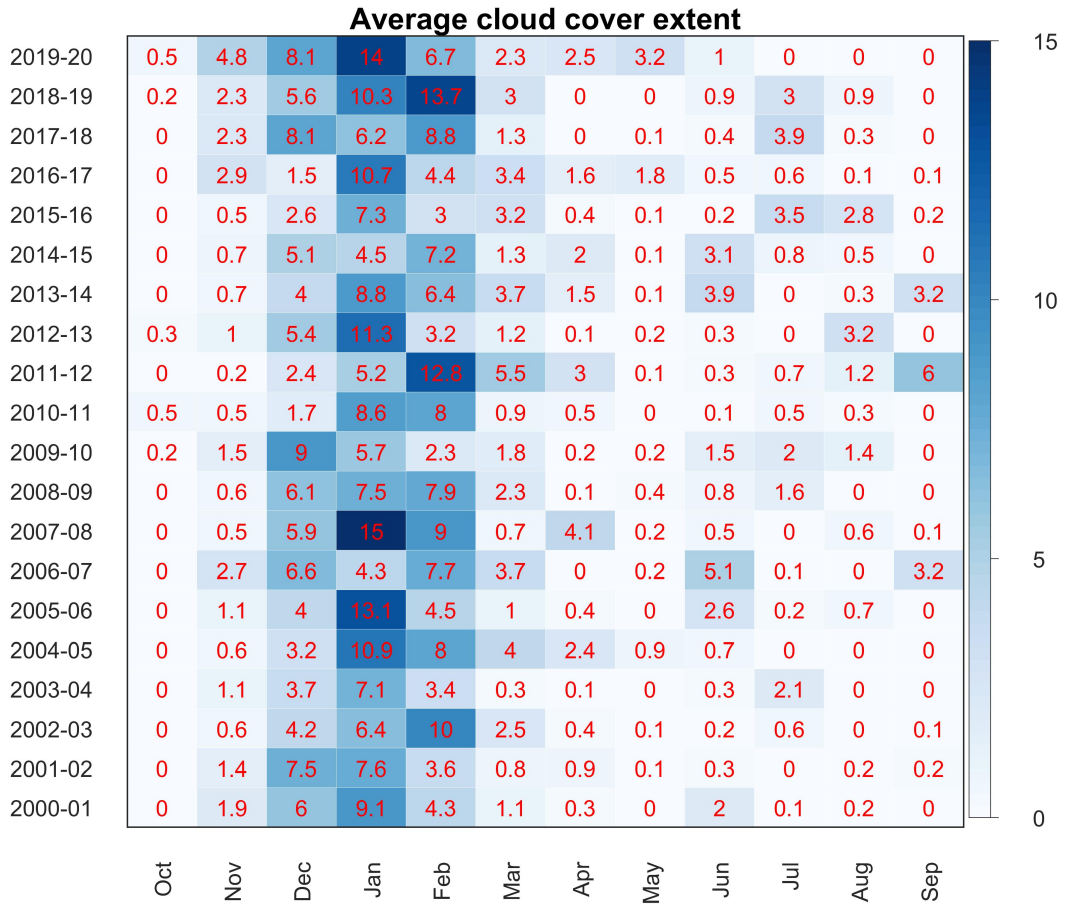

Figure 4.2: Average cloud cover extent in the analysis of monthwise variability in snow cover extent during 2000-2020

Across the entire study period, the snow cover extent follows a clear seasonal cycle, with minimum coverage during the late summer and early autumn months (August–October) and maximum coverage during the winter and early spring months (January–April). The monthly averages across the years indicate that February exhibits the highest snow cover, averaging 91%, followed by March (95%) and April (93%), reflecting the peak accumulation phase when persistent low temperatures minimize snowmelt. Snow cover begins to reduce in May (79%) and continues to decline through June (54%) and July (29%), reaching a minimum in August (24%), primarily due to increased temperatures and intensified ablation.

A gradual increase begins in September (31%) and becomes more pronounced in October (46%) and November (63%), indicating the onset of seasonal snowfall and accumulation.

On an interannual scale, the average annual snow cover across glaciological years ranges from a minimum of 55% (2011–2012) to a maximum of 74% (2009–2010), with the 20-year mean snow cover extent computed at 64%. The year 2009–2010 recorded consistently high snow cover values across nearly all months, with near-complete coverage observed from December to April, suggesting a particularly strong accumulation phase. Similarly, the glaciological years 2004–2005, 2008–2009, 2010–2011, and 2018–2019 also demonstrate above-average snow cover, particularly during the winter and early spring months, contributing to robust snowpack development.

Conversely, lower snow cover years such as 2011–2012 and 2016–2017 display reduced snow accumulation and early ablation signatures, especially evident in the significantly lower coverage during January and February. These years likely reflect either below-normal snowfall events or anomalous warming trends, which can influence water availability in the subsequent melt season. Notably, the year 2016–2017 exhibits a sharp increase from relatively low early-season values in October (24%) and November (32%) to peak values in February (96%) and March (97%), suggesting delayed but intense snowfall events.

Snow cover during March–May remains consistently high across most years, reinforcing the importance of this period for snow storage before the onset of melt. The transitional months of May and June show significant interannual variability, influenced by both melt onset timing and annual temperature fluctuations. For example, June snow cover ranged from as low as 37% (2017–2018) to as high as 77% (2009–2010), indicating the sensitivity of this period to climatic perturbations.

This analysis reveals the strong seasonality and interannual fluctuations of snow cover extent in the ZRB. Such variability has direct implications for regional water resources, glacier mass balance, and downstream hydrological regimes.

The findings underscore the need for sustained satellite monitoring and climate-adaptive water management strategies, particularly in the context of ongoing climatic changes impacting the cryosphere in the western Himalayas.

4.3 Impact of Climate Change

The ERA5-Land reanalysis data were utilized to derive regional mean monthly climatology over 1950-2020, specifically focusing on mean monthly precipitation and mean monthly temperature. These climatological signatures are presented in Table 4.4, Figure 4.3 and Figure 4.4, respectively, offering a detailed depiction of long-term climatic signals in the study region.

Table 4.4 Longterm mean monthly temperature and precipitation

Month	Mean monthly temperature (°C)	Mean monthly precipitation (mm)
October	-8.1	29.6
November	-15.7	28.4
December	-20.6	47.7
January	-23.1	73.3
February	-21.3	84.6
March	-17.5	98.7
April	-12.8	69.9
May	-7.7	51.4
June	-1.5	39.6
July	4.2	85.1
August	4.9	83.1
September	0.5	49.4
Annual Mean	**-9.9**	**61.8**

As detailed in Table 4.4, the Zanskar River Basin exhibits a characteristic cold desert climate, with pronounced seasonal variability in both thermal and precipitation regimes. Analysis of mean monthly temperature and precipitation data reveals distinct hydroclimatic patterns critical to understanding the basin's cryospheric dynamics.

Thermal Regime: The annual mean temperature of -9.9°C confirms the basin's high-altitude periglacial environment. Monthly temperatures demonstrate strong seasonality:

- **Winter Extremes:** January emerges as the coldest month (-23.14°C), with the December-February period maintaining sub -20°C temperatures, indicative of persistent ground freezing conditions.
- **Summer Moderation:** July and August represent the thermal maxima (4.18°C and 4.86°C respectively), though notably lacking true summer conditions (>10°C).
- **Transition Periods**: Steep thermal gradients occur during spring (Mar-May) and autumn (Sep-Oct), with monthly increases/decreases exceeding 4°C.

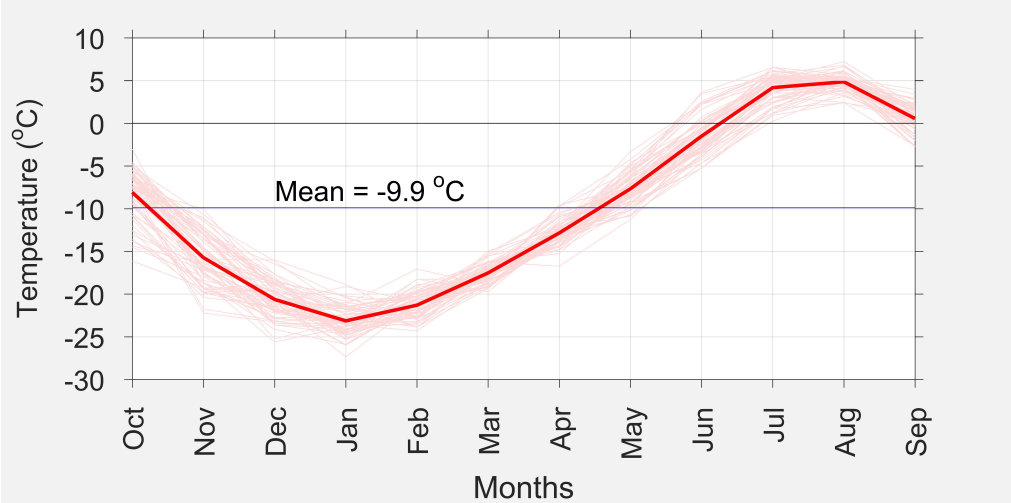

Figure 4.3: Mean monthly temperature variation of the ZRB as revealed by ERA5 monthly data during 1950-2021

Precipitation Distribution: The mean monthly precipitation of 62 mm reflects the basin's cold and semi-arid nature, with notable intra-annual variation:

- **Winter Dominance:** Three months of Jan-Mar receive peak precipitation

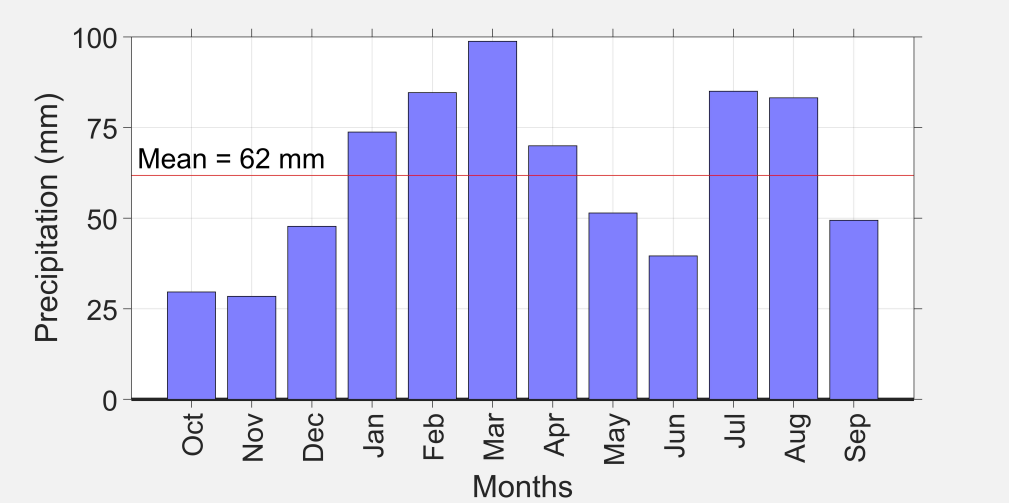

Figure 4.4: Mean monthly Precipitation pattern of the ZRB as revealed by ERA5 monthly data during 1950-2021

(257 mm), coinciding with westerly disturbance activity. The solid fraction likely dominates given subfreezing temperatures.

- **Secondary Summer Peak:** Jul-Aug precipitation (168 mm) suggests monsoon penetration, though with lower intensity than Himalayan regions.
- **Dry Periods:** Oct-Nov and May-Jun represent transitional periods with reduced precipitation.

Hydrological Implications: The phase partitioning of precipitation has significant cryospheric impacts:

- **Winter Accumulation:** Cold temperatures ensure snowpack preservation, contributing to seasonal water storage.
- **Summer Ablation:** Limited positive-degree days restrict meltwater generation, maintaining glacier mass balance.
- **Intra-annual Variability:** The bimodal precipitation distribution creates complex runoff timing, affecting downstream water availability.

The data underscore the basin's vulnerability to climate change, where minor temperature increases could significantly alter snow-rain partitioning and melt regimes. These findings provide critical baseline data for studying the regional climatology and modeling cryosphere-hydrology interactions in this sensitive high-mountain system. Therefore, the climatological data were analyzed at multiple temporal scales to assess both long-term and short-term trends, providing a comprehensive understanding of climatic variability and its impacts on snow cover dynamics. This included an evaluation of the long-term series spanning 1950–2020, as well as shorter 30-year climatic windows for the periods 1951–1980, 1961–1990, 1971–2000, 1981–2010, and 1991–2020. Additionally, a 5-year moving window analysis was conducted to examine changes in the rolling mean over the study period. These analyses were performed at both grid-wise and regional scales to capture basin-specific responses as well as broader regional distribution patterns. Special emphasis was placed on the summer season (May–Oct) to investigate changes in summer temperatures and snowfall over time, alongside an assessment of anomalies in positive degree days, which are critical drivers of snowmelt. The frequency of these anomalies was evaluated relative to the baseline period of 1961–1990. Furthermore, regional trends in snowfall were analyzed to understand how snowfall patterns have changed on both annual and seasonal scales, with the summer (May–Oct) and winter (Nov–Apr) seasons examined separately. Regional snowfall anomalies were also computed to quantify shifts in snowfall patterns relative to the baseline period, offering insights into the evolving climatic influences on snow cover dynamics. The findings of these analysis of temperature and snowfall time series are discussed in subsequent sections.

4.3.1 Snowfall

The Zanskar River Basin, situated in the cold and semi-arid trans-Himalayan region, exhibits a strongly seasonal precipitation regime characterized by distinct phase partitioning between rainfall and snowfall. The annual precipitation pattern demonstrates the basin's dual dependence on both winter snow accumulation and summer monsoon rainfall. Long-term precipitation characteristics in the ZRB pre-

sented in Table 4.5 and Figure 4.5 reveal an average annual total of 741 mm, with snowfall contributing approximately 500 mm (67% of total precipitation). This substantial proportion of solid precipitation underscores the basin's cryospheric dominance, where snow processes govern the regional hydrological regime. The 2:1 ratio of snowfall to rainfall highlights the critical role of winter accumulation in maintaining the basin's water resources, with implications for glacier mass balance and seasonal runoff patterns. The predominance of solid precipitation (particularly at elevations above 4,000 m) results in delayed water release through snowmelt, creating a vital natural storage mechanism that sustains river flow during dry periods. The high proportion of solid precipitation (particularly in winter months) sustains the basin's glaciers and provides gradual meltwater release. The sharp summer transition to liquid precipitation creates a bimodal hydrological regime with implications for water resource management. Analysis of monthly data reveals several key features of the basin's precipitation dynamics.

Table 4.5 Mean monthly precipitation, snowfall, and snowfall percentage

Month	Precipitation (mm)	Snowfall (mm)	Snowfall Percentage
January	73.7	70.4	96
February	84.6	79.2	94
March	98.8	89.8	90
April	69.9	62.6	88
May	51.4	40.4	79
June	39.6	18.5	47
July	85.0	15.9	19
August	83.2	8.8	11
September	49.4	21.1	43
October	29.7	23.5	79
November	28.5	26.3	92
December	47.8	45.4	95
Annual	741.6	500	67

- **Winter Dominance of Solid Precipitation (Dec−Feb):** During the winter months, precipitation occurs almost exclusively as snow, with snowfall accounting for 94-96% of total precipitation. January receives 73.7 mm total

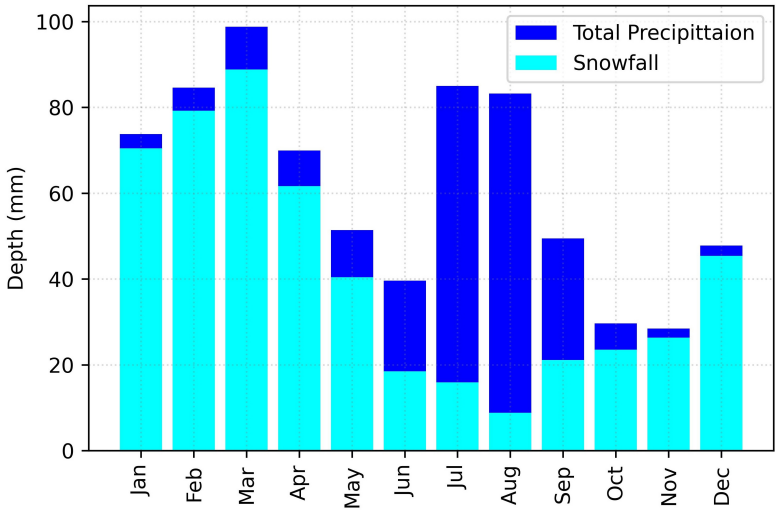

Figure 4.5: Total precipitation vs Snowfall (averaged over 1951-2020)

precipitation, of which 70 mm (96%) falls as snow. This period is critical for seasonal snowpack accumulation, which serves as the primary water storage mechanism in this high-altitude basin.

- **Transition Period (Mar−May):** The spring months show a gradual transition from snow-dominated to mixed precipitation. While March still maintains 90% snowfall contribution (89 mm of 98.8 mm total), this declines to 79% by May (40 mm of 51.4 mm total). This transition reflects increasing temperatures and marks the beginning of the snowmelt season, which provides essential water inputs prior to monsoon arrival.

- **Monsoon Influence (Jun−Sep):** The summer months exhibit a dramatic shift in precipitation phase. June shows near-equal partitioning (47% snowfall), while July and August become strongly rain-dominated, with only 19% and 11% snowfall contribution respectively. Despite being the warmest months, they receive the highest total precipitation (85.0 mm in July, 83.2 mm in August), primarily as rainfall associated with the Indian Summer Monsoon.

- **Autumn Transition (Oct−Nov):** Autumn marks a rapid return to snow-dominated precipitation, with October showing 79% snowfall (24 mm of 29.7 mm total) and November 92% (26 mm of 28.5 mm total). This transition

occurs as temperatures drop below freezing, re-establishing the winter snow accumulation regime.

The pronounced seasonality in precipitation phase has several important consequences. First, the winter snowpack acts as a natural water reservoir, with gradual melt maintaining baseflow during dry periods. Second, the high snowfall percentage (annual average ∼70%) contributes significantly to glacier mass balance. Third, the summer rainfall events, while less frequent, can generate flash floods due to the basin's steep topography and limited soil water storage capacity.

To further investigate, analysis were carried out to understand the seasonal behavior of snowfall, specifically summer (May–Oct) and winter (Nov–Apr) snowfall, along with annual snowfall patterns. Given that snowfall constitutes a significant portion of the total precipitation, its changing pattern was evaluated in terms of anomalies—deviations and directional trends. Since the rising temperatures directly impact snowfall, leading to its reduction and altering its pattern, liquid precipitation was excluded from subsequent analyses.

4.3.1.1 Snowfall anomaly

To assess the variation in snowfall patterns over ZRB, snowfall anomalies were calculated relative to the baseline period (1961–1990), a widely adopted reference period in climatological studies. The anomaly was computed for annual, summer, and winter snowfall to understand deviations from the historical norm, as illustrated in Figure 4.6. The analysis of snowfall anomalies reveals notable variability across annual, summer, and winter seasons. The post-2000 period, in particular, exhibits distinct trends compared to preceding decades, suggesting potential climatic shifts in the early 21st century. The anomalies for each season, emphasizing the frequency and magnitude of negative anomalies in the 2001–2020 period compared to earlier 20-year intervals (1951–1970, 1961–1980, 1971–1990, 1981–2000) are discussed below.

Annual snowfall anomalies: The annual snowfall anomalies in ZRB demon-

strate considerable interannual variability, with alternating phases of positive and negative deviations. However, the post-2000 period (2001–2020) stands out due to a pronounced increase in the frequency and intensity of negative anomalies.

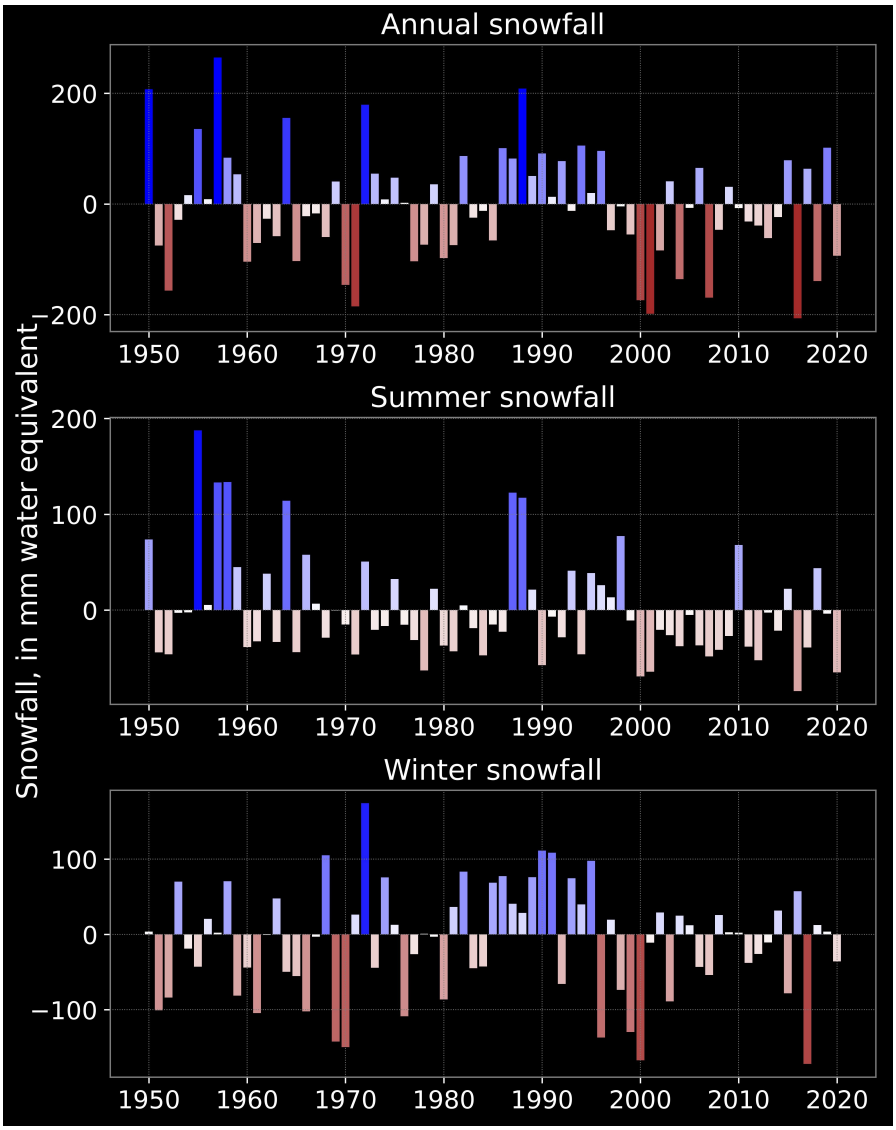

Figure 4.6: Anomaly in regional snowfall w.r.t. baseline period: 1961-1990

- **Pre-2000 Periods:**
  - **1951–1970:** Negative anomalies occurred in 12 out of 20 years (60%), with the most extreme being -146.2 mm w.e. (1970).

  - **1961–1980:** Negative anomalies were observed in 12 out of 20 years (60%), with the lowest being -184.9 mm w.e. (1971).
  - **1971–1990:** Negative anomalies were recorded in 8 out of 20 years (40%), with the most severe being -184.9 mm w.e. (1971).
  - **1981–2000:** Negative anomalies occurred in 9 out of 20 years (45%), with the lowest being -173.7 mm w.e. (2000).

- **Post-2000 (2001–2020):** Negative anomalies dominated, occurring in 14 out of 20 years (70%), with extreme deficits such as -206.6 mm w.e. (2016) and -198.5 mm w.e. (2001). The magnitude of negative anomalies post-2000 was more severe than in previous decades, with five years exceeding -100 mm w.e. compared to only sporadic instances in earlier periods. This shift suggests an intensification of snowfall deficits in the early 21st century, possibly linked to regional warming or changes in atmospheric circulation patterns.

Winter Snowfall Anomalies : Winter snowfall is critical for water storage in the ZRB, and anomalies in this season have significant hydrological implications. The post-2000 period exhibits a higher prevalence of negative anomalies compared to earlier decades.

- **Pre-2000 Periods:**
  - **1951–1970:** Negative anomalies occurred in 14 out of 20 years (70%), with the most extreme being -149.6 mm w.e. (1970).
  - **1961–1980:** Negative anomalies were observed in 13 out of 20 years (65%), with the lowest being -149.6 mm w.e. (1970).
  - **1971–1990:** Negative anomalies were recorded in 7 out of 20 years (35%), with the most severe being -108.6 mm w.e. (1976).
  - **1981–2000:** Negative anomalies occurred in 7 out of 20 years (35%), with the lowest being -167.3 mm w.e. (2000).

- **Post-2000 (2001–2020):** Negative anomalies were frequent, occurring in 10 out of 20 years (50%), with extreme deficits of -172.1 mm w.e. (2017). While the frequency is comparable to earlier periods. The persistence of strong negative anomalies in winter snowfall post-2000 may indicate a weakening of westerly disturbances or rising temperatures leading to reduced snow accumulation.

Summer Snowfall Anomalies : Summer snowfall anomalies, though generally smaller in magnitude than winter anomalies, also show a shift towards more frequent negative deviations in the 21st century.

- **Pre-2000 Periods:**
  - **1951–1970:** Negative anomalies occurred in 11 out of 20 years (55%), with the lowest being -46.1 mm w.e. (1952).
  - **1961–1980:** Negative anomalies were observed in 13 out of 20 years (65%), with the most extreme -63.0 mm w.e. (1978).
  - **1971–1990:** Negative anomalies were recorded in 13 out of 20 years (65%), with the lowest being -63.0 mm w.e. (1978).
  - **1981–2000:** Negative anomalies occurred in 11 out of 20 years (55%), with the most severe being -69.3 mm w.e. (2000).
- **Post-2000 (2001–2020):** Negative anomalies were more frequent, occurring in 17 out of 20 years (85%), with extreme deficits such as -84.6 mm w.e. (2016), -64.9 mm w.e. (2020) and -64.4 mm w.e. (2001). The post-2000 period also saw a higher frequency of years with deficits below -40 mm w.e. compared to earlier decades. This trend suggests a potential reduction in summer snowfall, possibly due to rising temperatures or shifts in monsoon-related precipitation patterns.

Notably, the magnitude of positive anomalies post-2000 have decreased in comparison to pre-2000 period for annual, summer, and winter snowfall, as shown in Figure 4.6.

4.3.1.2 Snowfall trend

The trend in annual, summer and winter snowfall across the ZRB was analyzed over multiple temporal scales to assess both long-term and decadal-scale variability. The primary analysis encompassed the entire 71-year period from 1950 to 2020, supplemented by five overlapping 30-year climate windows (1951–1980, 1961–1990, 1971–2000, 1981–2010, and 1991–2020) to evaluate temporal shifts in snowfall patterns. This multi-temporal approach facilitates the identification of both persistent and transitional trends while accounting for inherent climatic variability.

Annual snowfall trend:

Annual snowfall trends in longterm period and multiple overlapping climate windows are shown in Figure 4.7. Over the long-term period (1950–2020), the ZRB exhibited a spatially widespread negative trend in annual snowfall. However, statistical testing at the 5% significance level indicated that these trends were not significant, suggesting that while a declining pattern is evident, it does not yet surpass the threshold of robust statistical confidence. This finding implies that the observed reduction in snowfall may be part of natural variability rather than a statistically robust climatic shift.

The earliest 30-year window (1951–1980) similarly demonstrated a predominantly negative trend across the basin, though, like the long-term analysis, these trends lacked statistical significance at the 5% level. This consistency suggests that the mid-20th century was characterized by a period of declining snowfall, albeit within the bounds of natural climatic fluctuations. A notable shift occurred during the subsequent window (1961–1990), where a reversal in trend direction was observed, with snowfall exhibiting an increasing tendency across much of the region. Notably, the southwestern and northeastern peripheries of the basin displayed statistically significant positive trends, indicating localized zones of increasing snowfall accumulation. Within the central basin, isolated pockets also exhibited significant increases, though the broader basin-wide trend, while positive, did not uniformly meet the threshold for statistical significance.

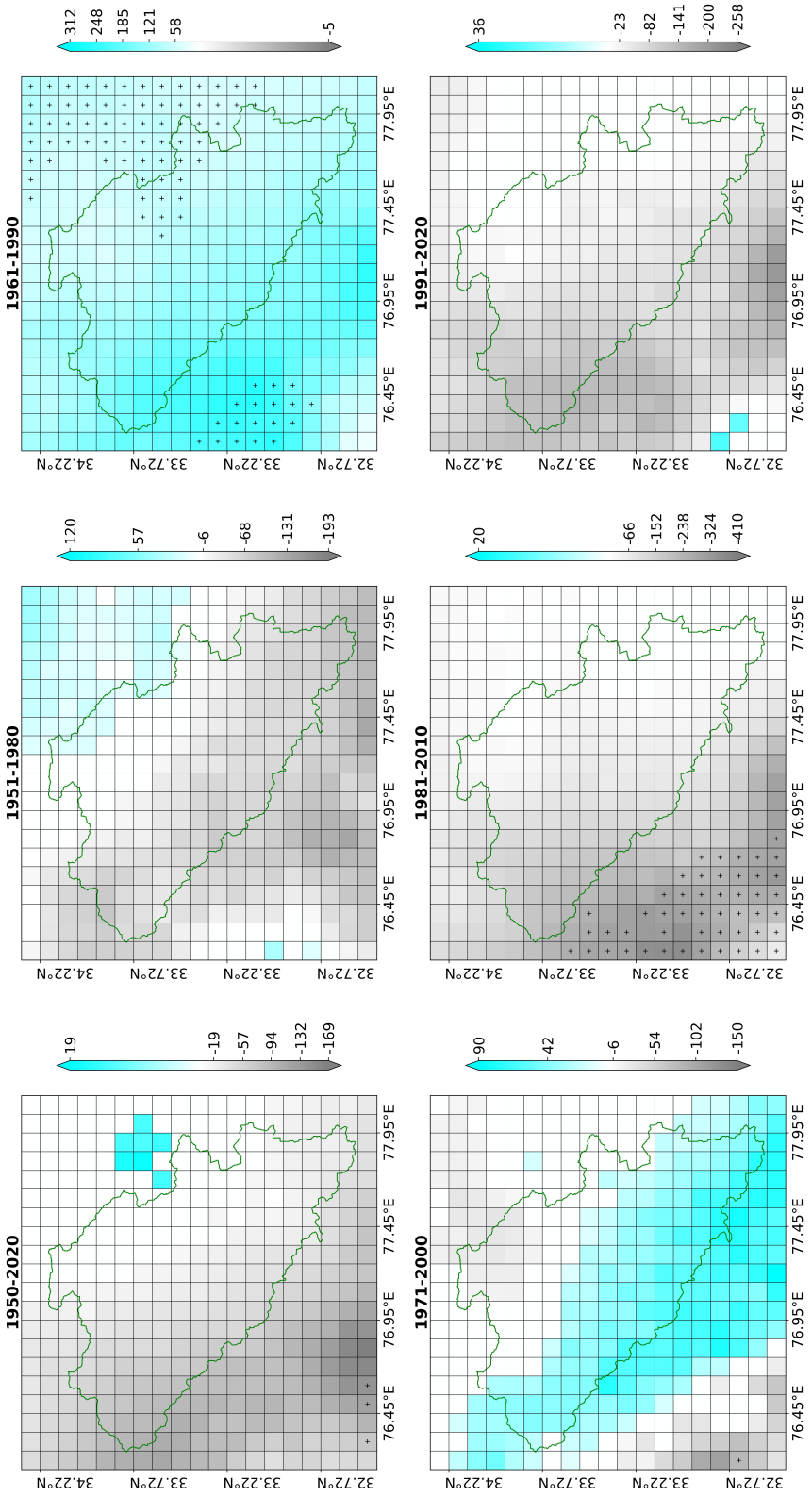

Figure 4.7: Trend in annual snowfall; significant trends at the 5% significance level are shown with dots (units in mm w.e.)

The following period (1971–2000) was marked by spatially heterogeneous trends, with a discernible increase along a northwest-southeast axis. Despite this regional coherence, none of the observed trends reached statistical significance, underscoring the variability inherent in snowfall patterns over this interval. A pronounced transition occurred in the 1981–2010 window, during which the basin experienced a reversal from previously positive to predominantly negative trends. The southwestern periphery of the basin emerged as an area of statistically significant decline, while regions within the basin, though exhibiting negative trends, were not found to be statistical significant. The most recent 30-year window (1991–2020) also showed spatially extensive negative trends across the ZRB. However, as with earlier periods, these trends did not attain statistical significance at the 5% level. The persistence of negative trends across multiple temporal scales, particularly in recent decades, raises important questions regarding potential climatic influences, including rising temperatures and shifting atmospheric circulation patterns. The absence of statistical significance in the most recent window may reflect either the high natural variability of snowfall or the early stages of a more sustained decline that has yet to surpass detection thresholds.

Summer snowfall trend:

Summer snowfall trends in longterm period and multiple overlapping climate windows are shown in Figure 4.9. During the long-term period (1950–2020), a widespread negative trend was observed across the basin, with statistically significant declines (5% level) concentrated along the northwest-southeast axis. This pattern indicates reduction in summer snowfall across much of the region, though isolated pockets in the northeastern sector exhibited particularly strong declines. For the period 1951–1980, summer snowfall trends were predominantly negative throughout the ZRB, though none reached statistical significance at the 5% level except in the southeastern sector. The subsequent window (1961–1990) exhibited a contrasting spatial pattern, with positive trends emerging in the northeastern basin—indicating a temporary increase in summer snowfall—while the remainder of the region continued to experience nonsignificant negative trends. A notable reversal occurred during 1971–2000, with trends opposing those of the preceding 1961–1990 period, though statistical significance remained absent.

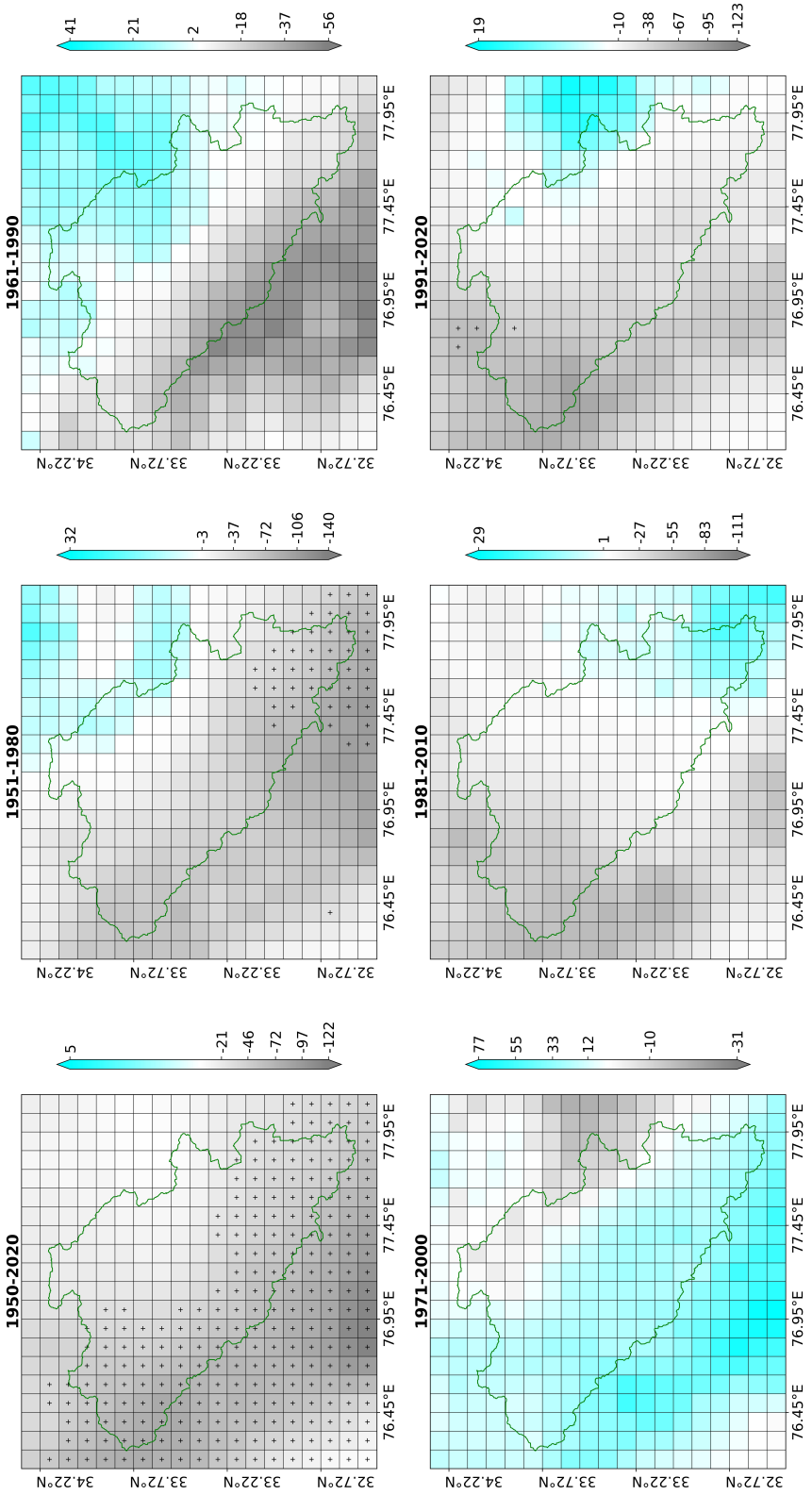

Figure 4.8: Trend in summer snowfall; significant trends at the 5% significance level are shown with dots (units in mm w.e.)

From 1981 to 2010, negative trends dominated again, with the exception of isolated pockets in the southeastern basin where slight increases were detected. However, as in earlier intervals, these trends lacked statistical significance, underscoring the challenge of detecting robust signals amid high interannual variability.

The most recent climatic window (1991–2020) demonstrates a pronounced and spatially coherent negative trend, with statistically significant declines (5% level) localized to one grid cell within the basin and three adjacent to it.

Winter snowfall trend:

Winter snowfall trends in longterm period and multiple overlapping climate windows are shown in Figure 4.9. During the long-term period (1950–2020), winter snowfall exhibited a widespread positive trend across the basin, contrasting sharply with the negative trends observed in summer snowfall during the same period. However, these positive trends failed to attain statistical significance at the 5% level, indicating that while the directional pattern suggests increased winter snowfall, the changes are not robust enough to reject the null hypothesis of no trend.

The earliest climatic window (1951–1980) displayed mixed trends, with a predominance of negative trends across the ZRB. Similar to the long-term trend, these variations were not statistically significant, suggesting that the observed declines were not systematic enough to be distinguished from natural variability. A notable shift occurred during the 1961–1990 period, when the entire basin exhibited statistically significant positive trends at the 5% significance level. This pattern stands in stark contrast to the concurrent summer snowfall trends, which were predominantly negative, highlighting a seasonal divergence in snowfall response to climatic drivers during this interval. Subsequent decades demonstrated a reversal of this pattern. The 1971–2000 window showed a decline in winter snowfall relative to the previous period, though the trends remained statistically insignificant. The following climatic window (1981–2010) continued this pattern but introduced a new spatial nuance: a strong negative trend emerged at the south-east of the ZRB, though the negative trends within the ZRB remain statistically non-significant.

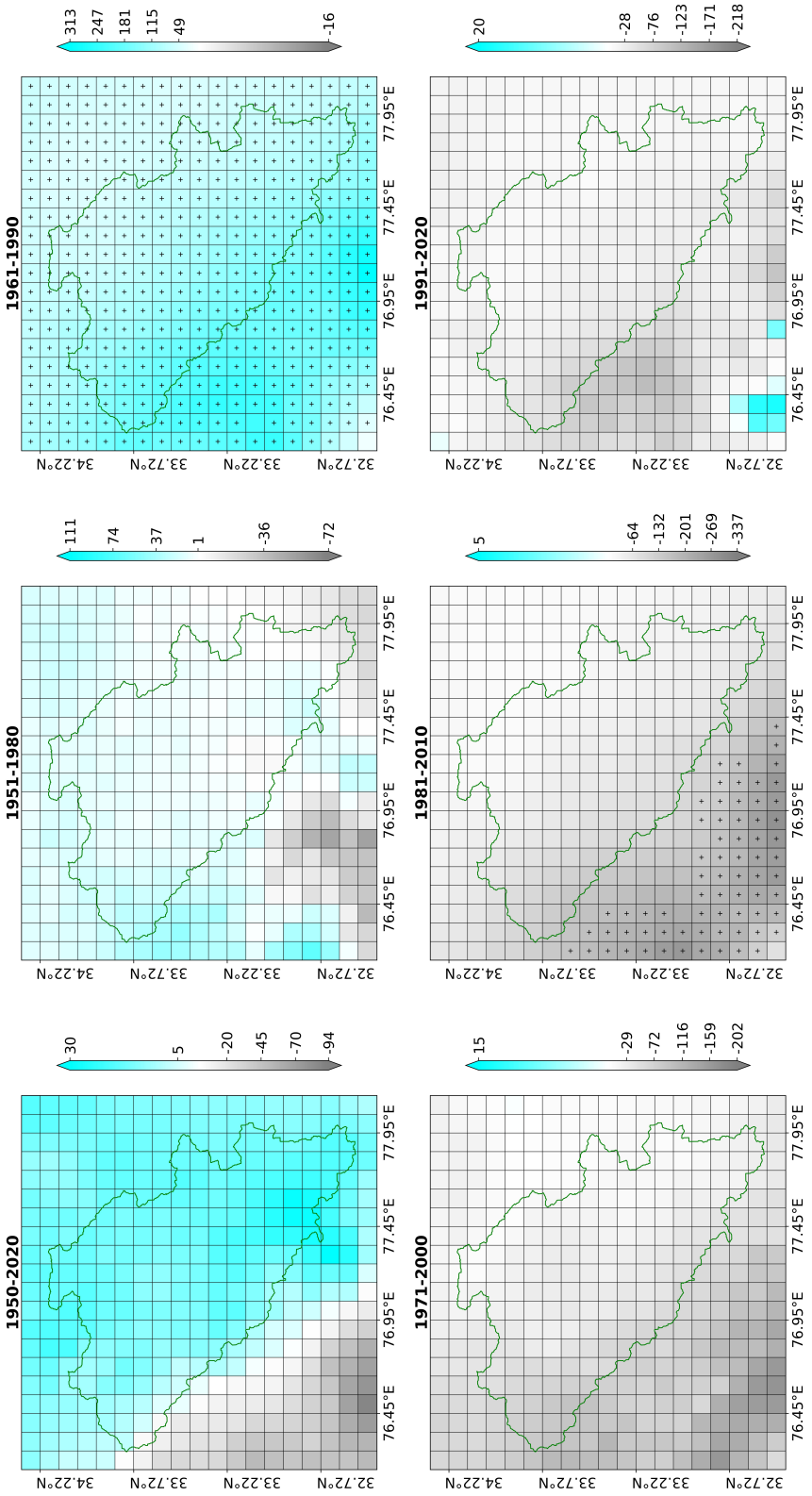

Figure 4.9: Trend in winter snowfall; significant trends at the 5% significance level are shown with dots (units in mm w.e.)

The most recent period (1991–2020) exhibited a predominantly negative trend in winter snowfall, however, none of the grid-level trends reached statistical significance, implying that while the directional signal suggests a reduction in winter snowfall, the magnitude of change remains within the bounds of climatic noise. This absence of significant trends in recent decades, despite the apparent negative tendency, may reflect either increased variability in winter precipitation regimes or the influence of localized atmospheric processes that are not yet strong enough to produce statistically detectable trends.

4.3.1.3 Snowfall trend in 5 year moving window

One of the most effective methods for assessing the direction of climate change is trend analysis using a moving window approach. In this study, spatial snowfall trends were also analyzed using a 5-year moving window from 1950 to 2020 (Figure 4.10).

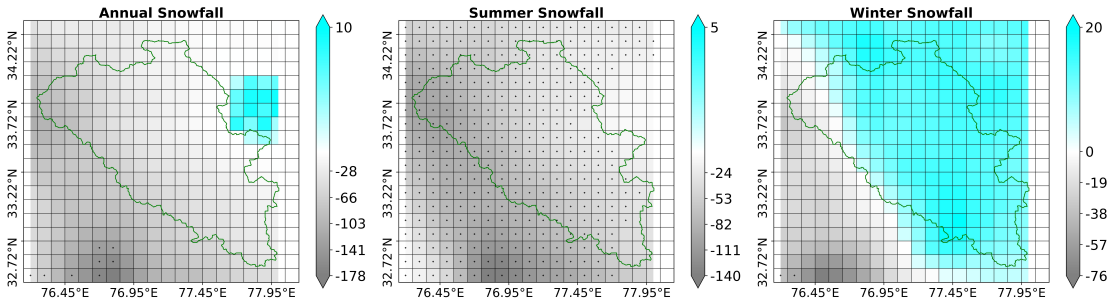

Figure 4.10: Trend in snowfall in 5 year moving window, (units in mm, w.e.)

For annual snowfall, the majority of grid cells exhibited negative trends, indicating a general decline in snowfall accumulation over the study period. However, none of these trends reached statistical significance at the 5% level. Contrary to that, summer snowfall displayed a markedly different spatial signature, with widespread and statistically significant negative trends observed across much of the basin and surrounding region. These robust declines in summer snowfall likely reflect broader climatic shifts, such as rising temperatures that favor rain over

snow or alterations in atmospheric circulation patterns affecting moisture delivery during the summer months. The statistical significance of these trends underscores their climatic relevance and suggests that summer snowfall reductions may be a more sensitive indicator of regional climate change compared to annual totals.

In contrast to the annual and summer patterns, winter snowfall trends in the ZRB were predominantly positive, with only a limited number of grid cells showing decreases. However, similar to the annual trends, these winter patterns did not achieve statistical significance at the 5% level. The lack of statistical significance implies that these increases remain within the range of natural variability. This dichotomy between summer and winter trends highlights the seasonally divergent responses of snowfall to climatic changes in high-mountain environments, with summer snowfall exhibiting greater sensitivity to warming temperatures while winter accumulation shows more resilience or even potential increases in some areas. The absence of significant trends in annual totals despite strong summer declines further suggests that winter increases may be partially offsetting summer losses at the annual scale, though this compensation appears incomplete given the overall negative (albeit non-significant) annual trends. These findings emphasize the importance of considering seasonal snowfall trends separately to fully understand the complex spatial and temporal dynamics of cryospheric change in mountainous regions.

The analysis of snowfall trends was also conducted at regional scale by aggregating snowfall data across the entire study domain to assess regional-scale patterns (Figure 4.11). The findings reveal a consistent negative trend in snowfall across annual, summer, and winter season when analyzed using the 5-year moving window methodology. Notably, statistical testing of the long-term record (1950–2020) in moving window revealed that only the summer season exhibited a statistically significant trend at 5% significance level, confirming the robustness of this declining trajectory. This pronounced reduction in summer snowfall carries particular hydrological importance, as the six-month summer period typically contributes substantially to seasonal snowpack accumulation. The differential response between seasons - with summer showing significant declines while annual and winter trends, though negative, lack statistical significance - may reflect vary-

ing atmospheric drivers influencing precipitation patterns across different periods of the year. This seasonal asymmetry in snowfall reduction warrants further investigation to elucidate the underlying climatic mechanisms and improve predictive modeling of future water availability scenarios.

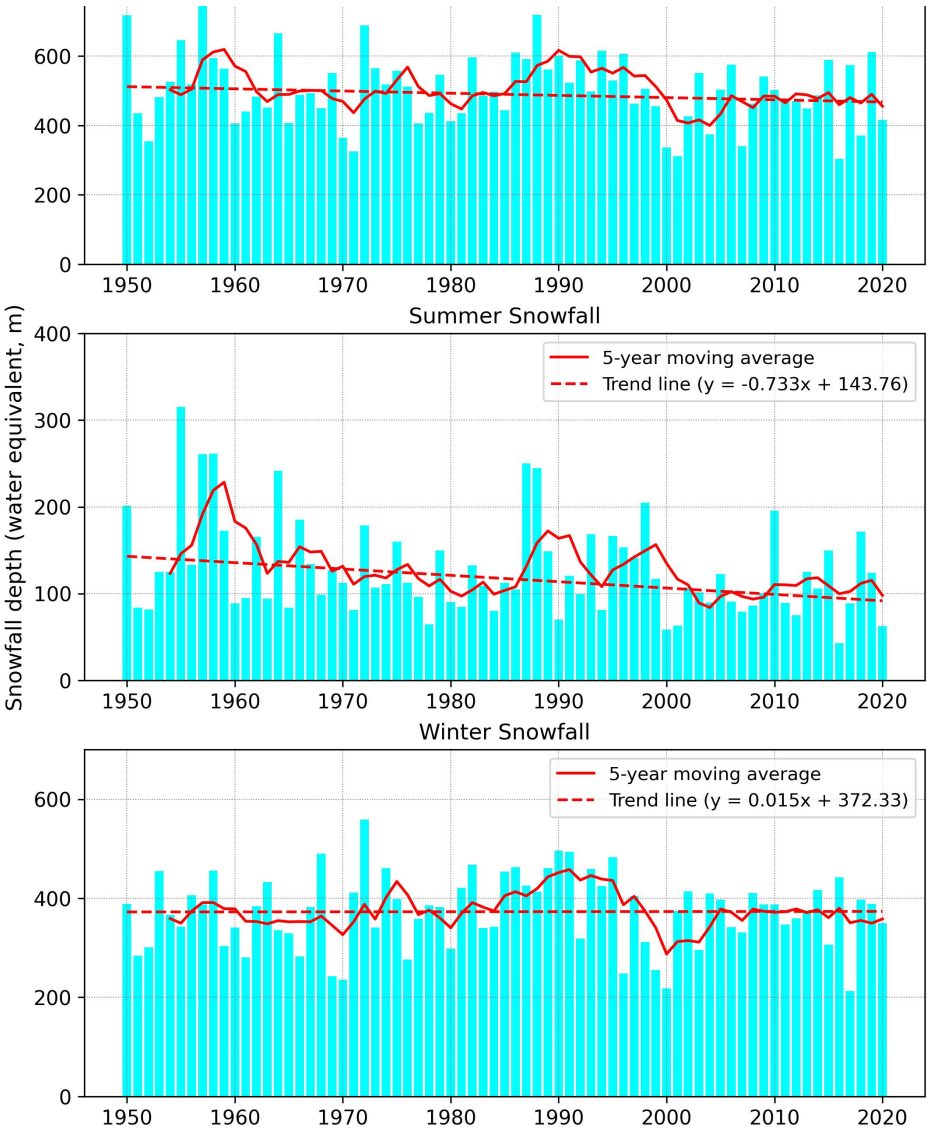

Figure 4.11: Regional trend in annual, summer and winter snowfall in 5-year moving window

4.3.2 Temperature

An analysis of ERA5 Land temperature data was carried out for the period 1950-2020. A subset of this data, spanning the first two decades of the 21st century (2000-2020), was further examined to determine the mean monthly temperature and its variability, as illustrated in Figure 4.12. The monthly temperature data for the ZRB from 2000 to 2020 reveal distinct seasonal patterns and interannual variability, characteristic of high-altitude Himalayan climates. The basin experiences pronounced thermal seasonality, with mean monthly temperatures ranging from extreme winter minima to moderate summer maxima.

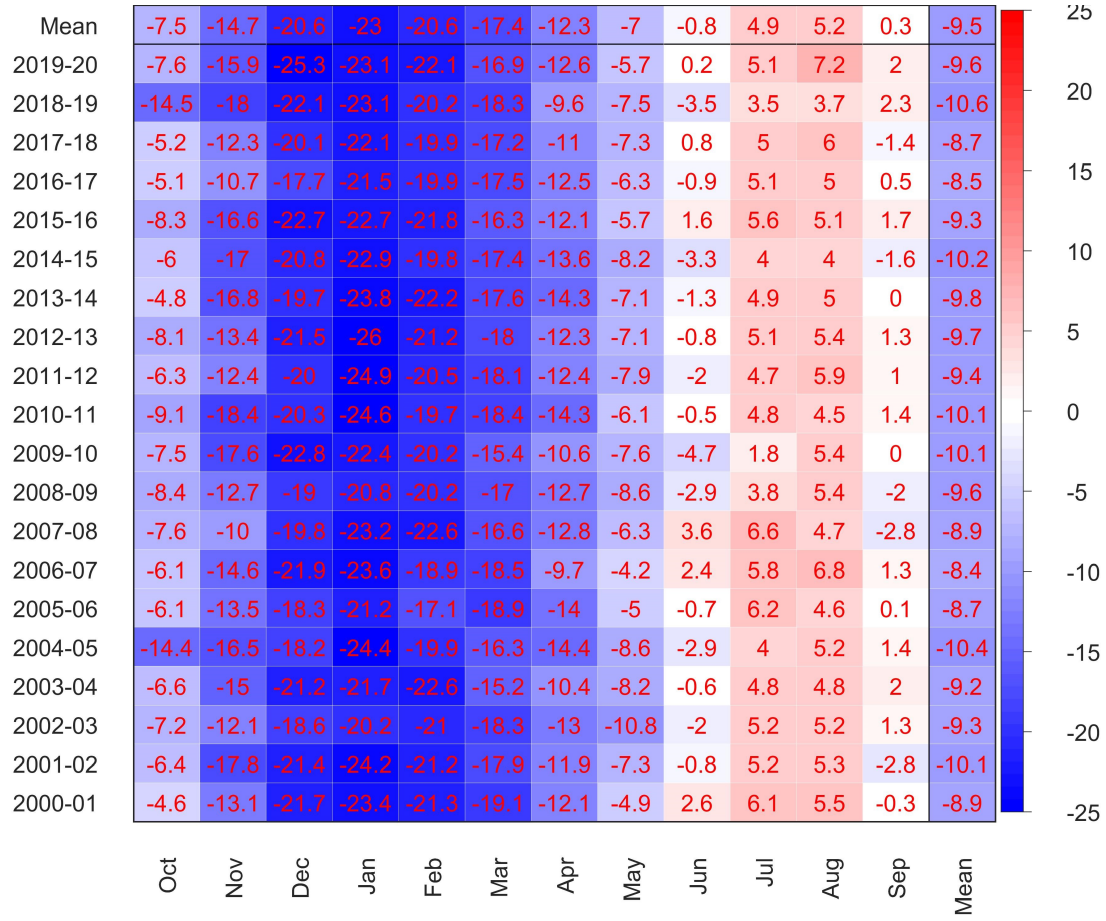

Figure 4.12: Regional trend in annual, summer and winter snowfall in 5-year moving window

During the winter months (Dec-Feb), temperatures remain consistently sub-zero, with January emerging as the coldest month (average: -23.0°). The December-February period exhibits minimal thermal variability, with mean temperature of -20.6°. The autumn transition (Oct-Nov) shows rapid cooling, with temperatures dropping from -7.5° in October to -14.7° in November as the region enters the winter regime.

The spring months (Mar-May) demonstrate a gradual warming trend, though temperatures remain below freezing until May (-7.0°). March (-17.4°) and April (-12.3°) exhibit slower warming rates compared to May, likely due to persistent snow cover albedo effects and latent heat consumption during melt processes. The summer phase (Jun-Aug) brings above-freezing conditions, with July (4.9°) and August (5.2°) as the warmest months. Notably, June (-0.8°) frequently records near-freezing temperatures, indicating delayed seasonal transitions typical of high-elevation environments.

Interannual variability is particularly evident in extreme monthly deviations, such as the anomalously cold October 2004 (-14.4°) or the warm September 2019 (2.3°). The annual average temperature (-9.5°) underscores the basin's cryospheric dominance, with 8 months averaging below freezing. These thermal characteristics have direct implications for glaciological and hydrological processes. The extended sub-zero period (Oct-May) facilitates seasonal snowpack accumulation, while the narrow summer ablation window (Jun-Sep) modulates meltwater contributions to the Zanskar River system. The observed interannual variability in transitional months (e.g., Apr, Oct) may influence the timing of spring melt onset and autumn snow accumulation, potentially affecting downstream water availability. The data provide a critical baseline for assessing climate change impacts on this sensitive cryospheric system.

Furthermore, to elucidate the temperature shift in the study area, an analysis of annual average mean temperature anomalies was performed relative to the 1961-1990 baseline period. This enabled an assessment of the magnitude and direction of annual temperature changes with respect to the reference period. The temperature anomaly analysis relative to the 1961–1990 baseline period highlights

a distinct warming trend, particularly in the post-2000 period (Figure 4.13). Over the decades, temperature anomalies have exhibited significant interannual variability, with alternating warm and cold deviations from the baseline. However, a clear shift towards more frequent and intense positive anomalies is evident in recent years, indicating an accelerated warming trend in the ZRB.

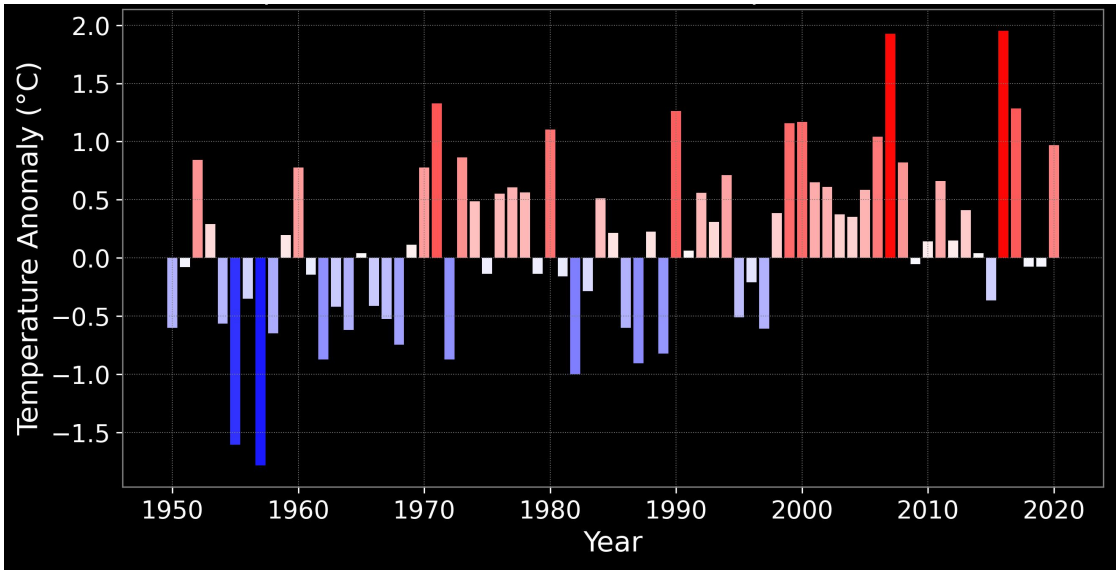

Figure 4.13: Anomaly in regional temperature w.r.t. baseline period: 1961-1990

The anomalies in annual average mean temperature for ZRB reveal distinct multidecadal variability with a pronounced shift toward warmer conditions in the 21st century. Relative to the baseline period (1961-1990), the data demonstrate an overall warming trend, particularly accentuated in the post-2000 period. During the second half of the 20th century (1950-2000), temperature anomalies exhibited considerable interannual variability, fluctuating between -1.78°C (1957) and +1.33°C (1971). The period featured alternating cool and warm phases, with no sustained multiyear warming trends. Notably, the 1950s and 1960s were predominantly cooler, with 60% of years showing negative anomalies, while the 1970s and 1980s displayed greater variability with intermittent warm years (e.g., 1980: +1.10°C). The 1990s marked a transitional period, with positive anomalies becoming more frequent (50% of years) and the decade ending with consecutive warm years (1999: +1.16°C; 2000: +1.17°C).

The post-2000 period (2001-2020) reveals a stark departure from historical patterns, with 85% of years exhibiting positive anomalies and several years exceeding +1.0°C (2006: +1.04°; 2007: +1.93°C; 2016: +1.95°C). This represents a doubling in the frequency of such extreme warm years compared to the previous five decades. The early 21st century warming is particularly evident in the increased occurrence of consecutive warm years - a phenomenon absent in earlier periods. For instance, 2001-2008 saw eight consecutive years with positive anomalies, unprecedented in the observational record. The magnitude of warming post-2000 is noteworthy, with the mean annual anomaly for 2001-2020 measuring +0.57°C compared to -0.01°C for 1950-2000. This 0.56°C increase is worrisome, suggesting elevation-dependent amplification characteristic of high-altitude regions. The warmest years on record (2007, 2016) both occurred in this period, with anomalies approaching +2.0°C - a threshold never reached in the 20th century for the ZRB. This accelerated warming in the early 21st century represents a climatic regime shift for the ZRB, with profound implications for cryospheric systems. The persistence of positive anomalies, particularly the emergence of multiyear warm sequences, suggests a transition toward a new climatic normal that may fundamentally alter the basin's hydrological functioning.

4.3.2.1 Temperature trend

To further investigate the warming pattern in the study region, a trend analysis of the annual mean temperature was conducted over the long-term period of 1950–2020 (70 years), as well as for multiple 30-year climatic windows, namely 1951–1980, 1961–1990, 1971–2000, 1981–2010, and 1991–2020 (Figure 4.14). The analysis of annual average mean temperature trends across the region from 1950 to 2020 reveals a prevalent and statistically significant ($p < 0.05$) increasing trend at every grid point. However, distinct temporal variations emerge when examining different 30-year climate windows. During the first climate window (1951–1980), a widespread increasing trend was observed, though statistical significance was predominantly confined to locations within the basin, with exceptions in the northern sector. Outside the basin, particularly in the western region, the trends, though positive, were not found to be statistically significant across all the grids.

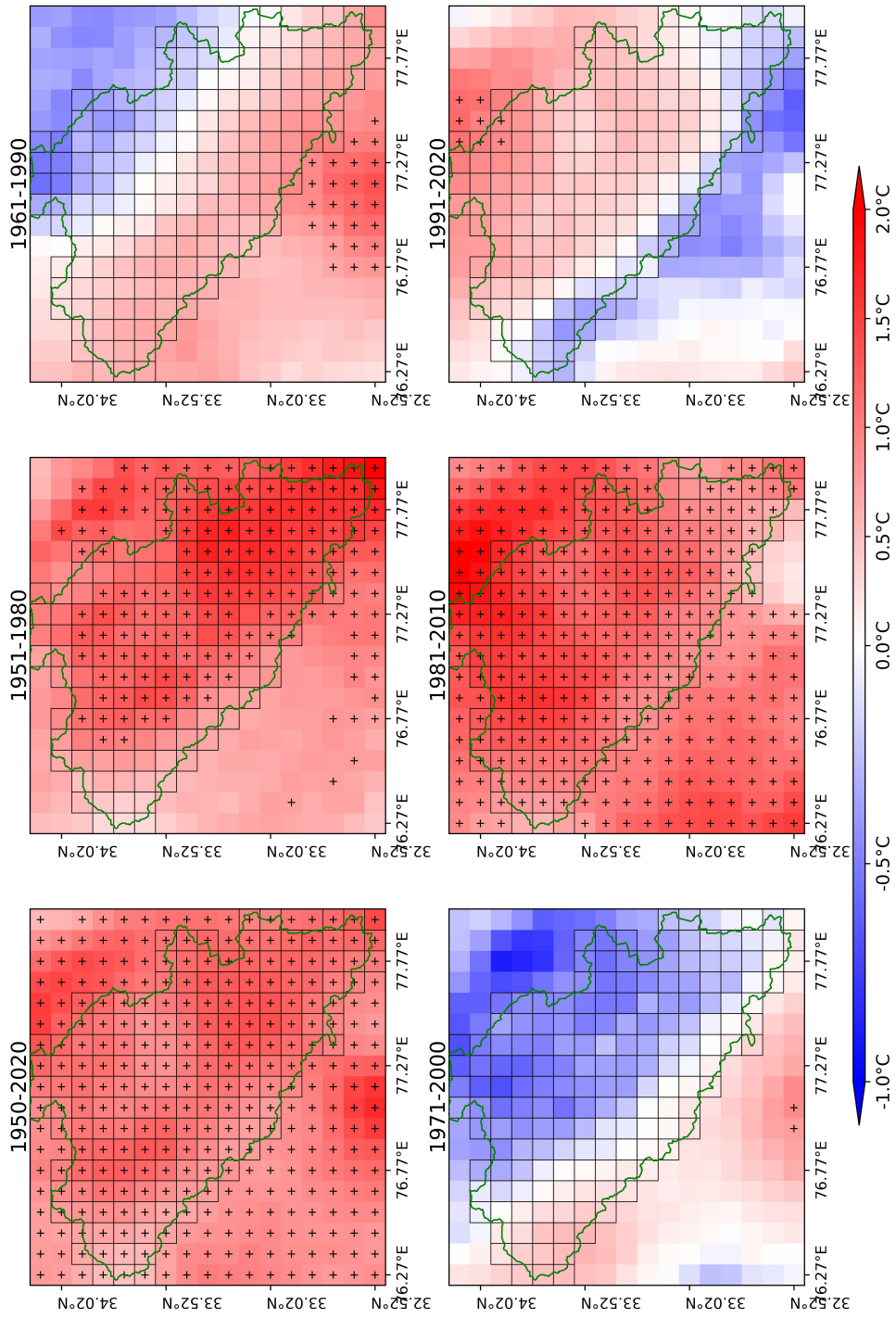

Figure 4.14: Trend in annual average mean temperature, significant trends at 5% significance level are shown with (+) sign

A notable reversal occurred in the subsequent window (1961–1990), where the northeastern part exhibited a declining trend in annual mean temperature. The basin itself displayed a mixed pattern, with temperatures decreasing to the right of southeastern to northwestern axis and increasing on the left side. This spatial heterogeneity intensified in the following period (1971–2000), with a pronounced cooling trend within the basin, though the changes were not statistically significant. A shift toward widespread warming was evident in the 1981–2010 window, where the entire basin and adjacent regions experienced statistically significant increasing temperature trends. However, the most recent climate window (1991–2020) exhibited a reversal of the 1961–1990 pattern, with temperatures increasing to the right the southeastern to northwestern axis and decreasing on the opposite side. Despite this shift, the trends were largely statistically non-significant.

Similar to annual average mean temperature, the analysis of trends in annual average summer mean temperature, comprising the months of May-Oct, across the ZRB revealed distinct temporal and spatial patterns over different climatic windows (Figure 4.15). From 1950 to 2020, a prevalent increasing trend was observed throughout the region, with the majority of grid points within the ZRB exhibiting statistically significant warming. When examining shorter 30-year climate windows, variations in trends became evident. During 1951–1980, a widespread but statistically non-significant warming trend was detected across the basin, with partial cooling observed in the northeastern sector. The subsequent period (1961–1990) exhibited stronger trends, with the previously noted cooling in the northeastern part of the basin becoming more pronounced. However, most trends within the basin remained statistically non-significant, and mixed signals were observed. The 1971–2000 window was characterized by widespread warming, though trends were predominantly non-significant. In contrast, the 1981–2010 period demonstrated prevalent warming, with a reasonably large number of grid points showing statistically significant trends both within and adjacent to the basin. The most recent climatic window (1991–2020) displayed a widespread increasing trend, with a considerable number of grid points exhibiting statistically significant warming. Interestingly, the spatial pattern of temperature changes in this period was nearly the reverse of that observed during 1961–1990, with non-

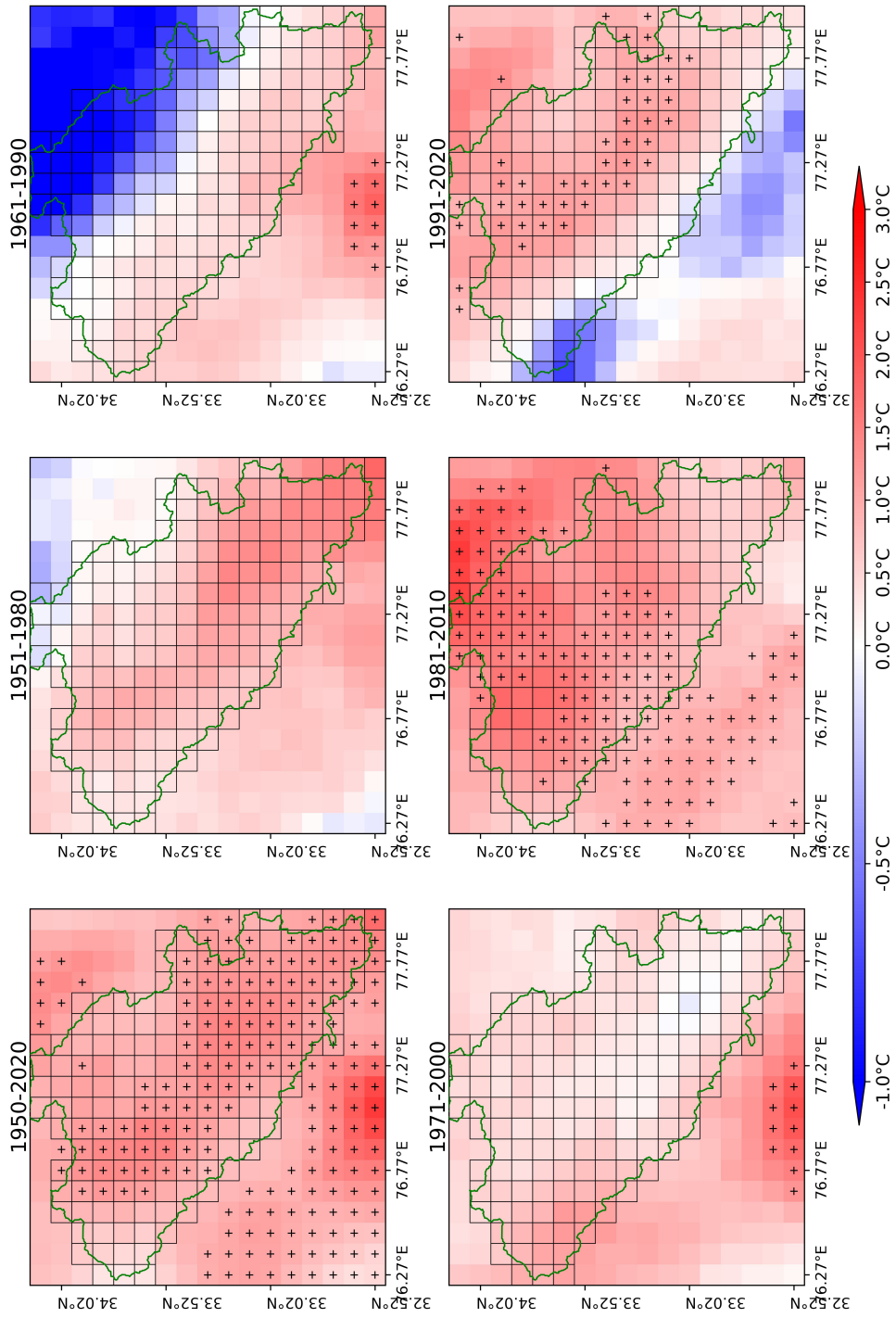

Figure 4.15: Trend in annual average summer mean temperature, significant trends at 5% significance level are shown with (+) sign

-significant cooling detected in the southwestern part of the basin—opposite to the earlier northeastern cooling trend.

These findings highlight the dynamic and non-uniform nature of temperature trends over the past seven decades, with alternating phases of warming and cooling, varying spatial patterns, and differing levels of statistical significance across different temporal segments.

4.3.2.2 Temperature trend in 5 year moving window

The analysis of gridwise trends over a five-year moving window revealed statistically significant warming patterns for both the annual average mean temperature and the annual average summer mean temperature (Figure 4.16). The results demonstrated widespread significant increases across every grid point at a 5% level of statistical significance. This indicates a robust and pervasive warming trend in both annual and summer mean temperatures. The consistency of these trends across all grid points underscores the broad spatial extent of the temperature changes, reinforcing the evidence of a systematic climatic shift.

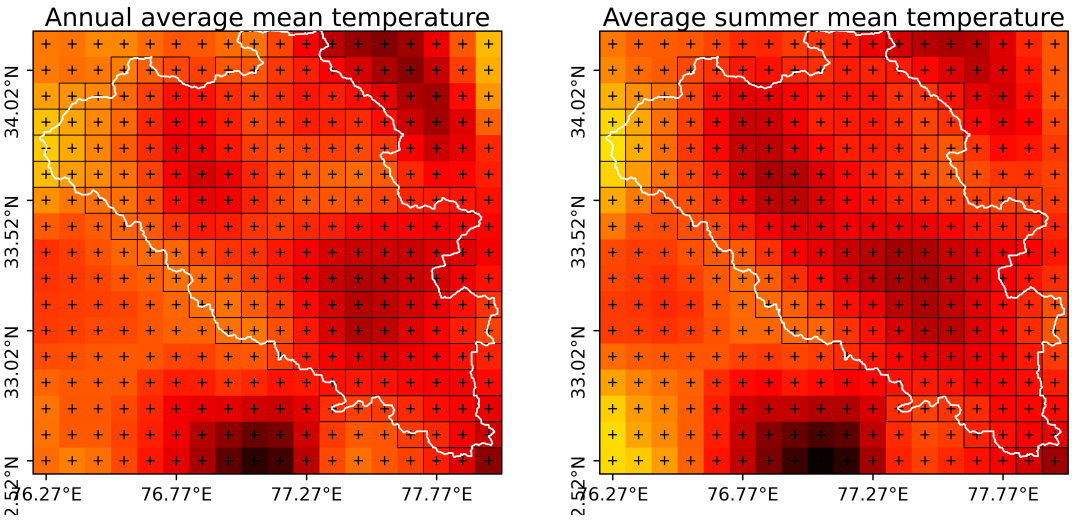

Figure 4.16: Temperature trend in 5 years moving window, significant trends at 5% significance level are shown with (+) sign

In addition to analyzing the spatial trends, the regional trends in the annual average mean temperature and the annual average summer mean temperature were examined by computing basin-wide averages. The results revealed statistically significant warming trends at 5% significance level for both the annual (Figure 4.17) and summer mean temperatures (Figure 4.18), indicating a pronounced warming in the region.

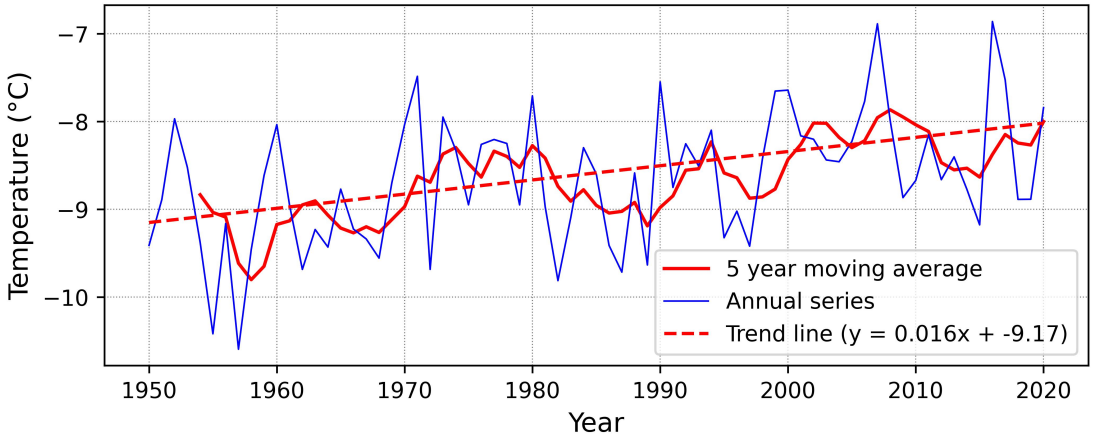

Figure 4.17: Regional trend in annual average mean temperature in 5-year moving window

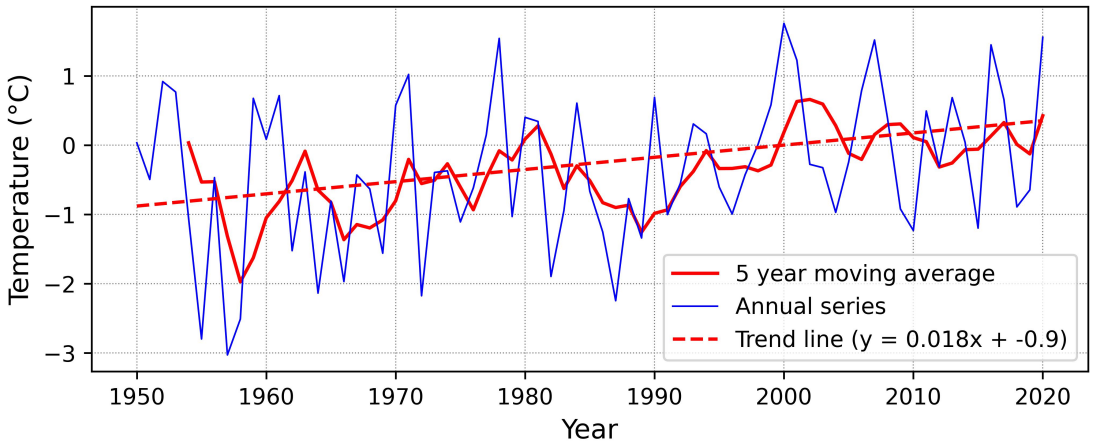

Figure 4.18: Regional trend in annual average summer mean temperature in 5-year moving window

4.3.2.3 Positive degree days

The analysis of Positive Degree Day (PDD) anomalies in the Zanskar River Basin reveals significant changes in thermal forcing patterns over the past seven decades. PDDs, calculated as the cumulative sum of daily temperatures above 2°C, show distinct temporal variations when comparing different climatological periods against the post-2000 era (Figure. 4.19).

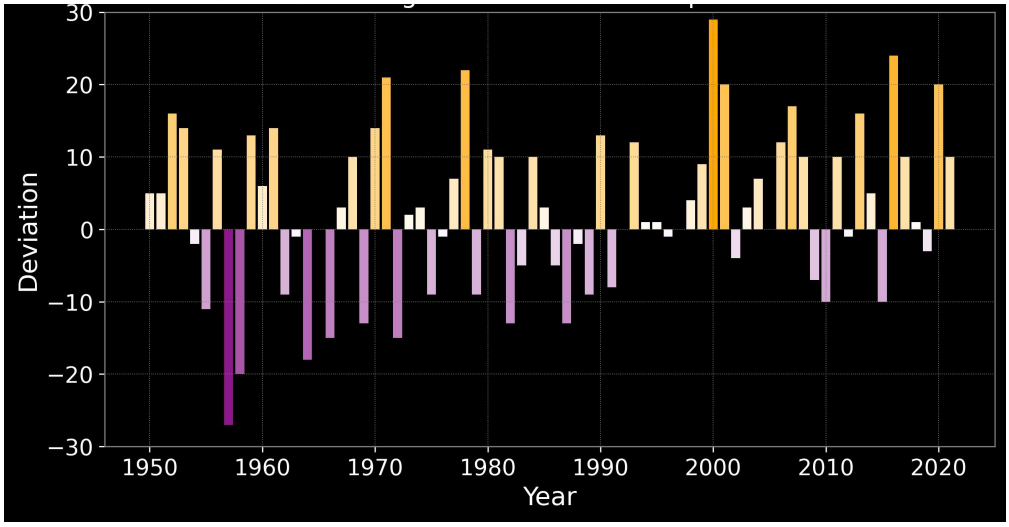

Figure 4.19: Anomaly in positive degree days (>2 °C) w.r.t. baseline period: 1961-1990

During the mid-20th century (1951-1970), PDD anomalies exhibited considerable interannual variability but remained near-neutral on average (-0.95 PDD). This period was characterized by alternating cold and warm phases, with notable extreme anomalies such as the record cold year of 1957 (-27 PDD) and the exceptionally warm year of 1978 (+22 PDD). The subsequent decades (1961-1980 and 1971-1990) maintained this pattern of variability, though with a gradual reduction in the frequency and intensity of negative anomalies. A clear transition became apparent in the 1981-2000 period, when the mean anomaly shifted to +1.8 PDD, marking the beginning of more persistent warm conditions. The 1990s in particular saw several years with substantial positive anomalies, culminating in the record warm year of 2000 (+29 PDD).

The post-2000 period stands in stark contrast to earlier decades. The mean anomaly increased dramatically to +6 PDD, with positive anomalies occurring more frequently than during 1951-1970. The magnitude of warm extremes intensified, with multiple years exceeding +20 PDD anomalies (2000: +29; 2001: +20; 2016: +24; 2020: +20), while cold anomalies became both less frequent and less severe.

These changes have important implications for the region's cryosphere and hydrology. The increased thermal forcing, particularly the concentration of extreme warm anomalies in recent decades, suggests accelerated glacier melt and altered meltwater timing. Such changes may significantly impact water availability and ecosystem dynamics in this sensitive high-altitude region. The transition from variable, near-neutral conditions in the mid-20th century to consistently warmer conditions in the 21st century underscores the basin's vulnerability to ongoing climate change and highlights the need for adaptive water resource management strategies.

To investigate further, the gridwise spatial trend analysis of PDDs exceeding 2°C was performed to evaluate regional distribution changes at a 5% significance level. During the extended 1950-2020 period, a widespread increasing trend in PDD was evident, though most trends within the basin lacked statistical significance. Notably, some location outside the ZRB did exhibit statistically significant warming trends. The 30-year climate windows of 1951-1980, 1961-1990, and 1971-2000 displayed mixed trend patterns, all of which remained statistically non-significant within the basin, except few grids in the western boundary of ZRB for 1971-2000 which showed statistically significant warming through increasing trend in PDD. A distinct shift occurred during 1981-2010, when the region experienced accelerated warming marked by a significant increase in PDD. This pattern persisted in the recent 1991-2020 climate window, where continued PDD increases reinforced the warming signal, though some statistically non-significant negative trends appeared in western areas outside the ZRB.

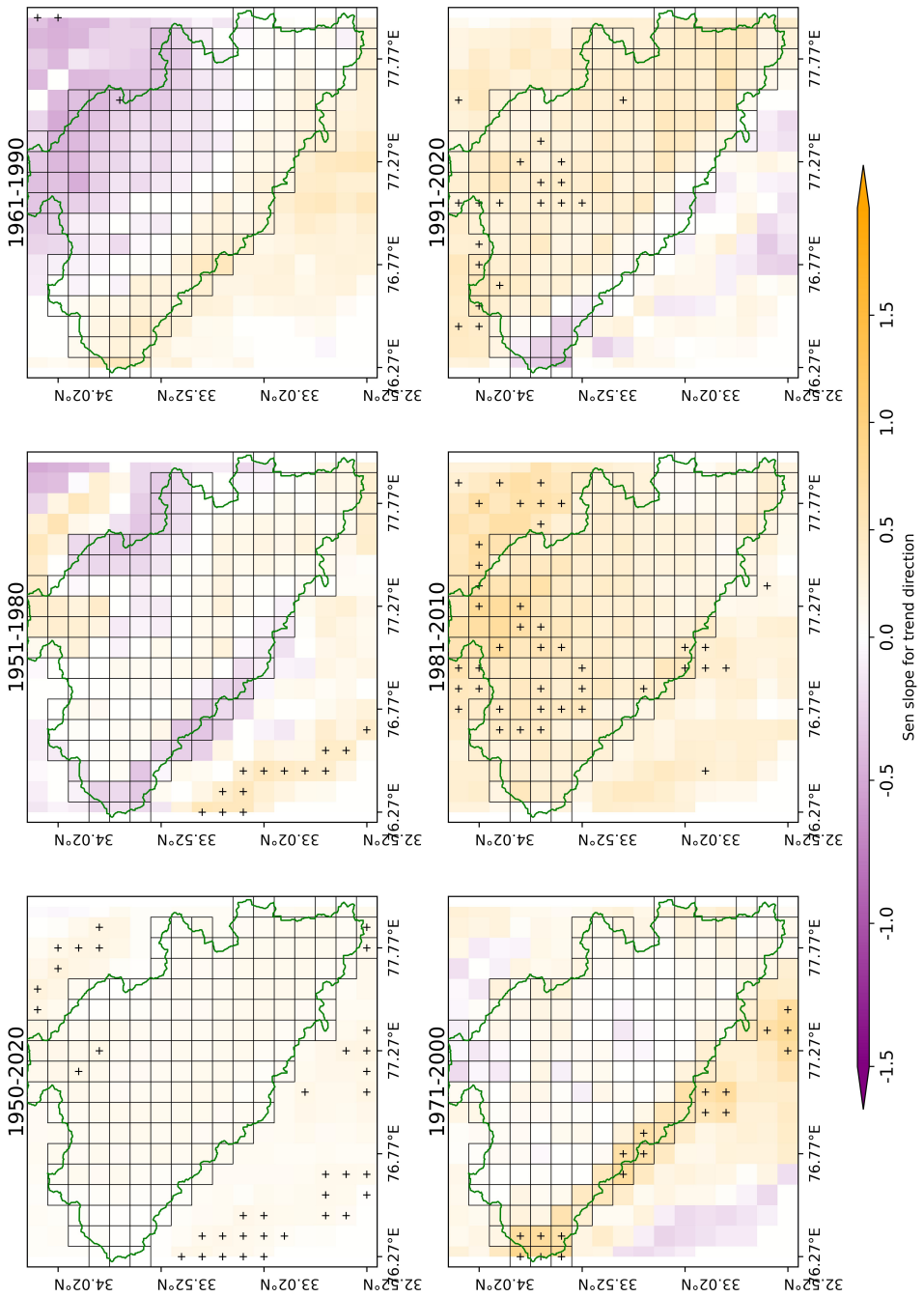

Figure 4.20: Trend in positive degree days (>2 °C) in summer season, significant trends at 5% significance level are shown with dots

Collectively, these findings demonstrate a long-term transition toward higher PDD values, with statistically significant warming trends initially concentrated outside the ZRB before becoming more prevalent within the basin during recent decades, consistent with broader climate change observations. The results highlight both the spatial heterogeneity and temporal progression of thermal regime changes across the study region.

Chapter 5

Summary and Conclusions

5.1 Overview

The Himalayan cryosphere, comprising extensive glaciers and ephemeral snow cover, plays a pivotal role in regional hydrology, yet its dynamics remain insufficiently understood due to sparse observational data. Snow cover serves as a critical freshwater reserve, modulating streamflow and groundwater recharge, particularly in the North Western Himalayas (NWH), where winter snowfall significantly contributes to river discharge. Traditional snow cover assessments face challenges such as logistical constraints and complex terrain, prompting reliance on satellite remote sensing. Since 2000, MODIS sensors aboard Terra and Aqua satellites have provided high-temporal-resolution snow cover products (e.g., MOD10A2/MYD10A2), enabling large-scale monitoring through indices like the Normalized Difference Snow Index (NDSI). However, accelerated glacial retreat linked to global warming underscores the urgency of understanding snow-climate interactions. While reanalysis datasets (e.g., ERA5-Land) offer valuable climate records, existing studies often neglect localized variations, particularly in high-altitude regions like the Zanskar River basin in Ladakh. Zanskar River Basin (ZRB), heavily reliant on snowmelt, lacks detailed assessments of spatiotemporal snow cover extent (SCE) and its climatic drivers, hindering accurate hydrological predictions. Key knowl-

edge gaps include topographic controls on snow distribution, intra-annual SCE variability, and long-term climate impacts. Addressing these through remote sensing and reanalysis data can refine snowmelt models and adaptation strategies.

Keeping above discussion in view, following specific objectives were formulated for this study,

1. To analyze the spatial distribution of snow cover extent in Zanskar River basin with respect to elevation, slope, and aspect.
2. To analyze the seasonal variability in snow cover extent in Zanskar River basin .
3. To investigate the impact of climate change on snow cover extent during 2001-2020.

This study employed a multi-faceted methodological approach to investigate snow cover dynamics in the ZRB using remote sensing, geospatial analysis, and climatological data. A total of 939 MODIS MOD10A2 eight-day composite snow cover products (2000–2020) from the TERRA satellite were analyzed at 500 m spatial resolution, capturing maximum snow extent defined as areas with snow presence during any day of the eight-day interval. Topographic stratification of the basin was performed using SRTM 90 m DEM-derived elevation, slope, and aspect maps to assess snow distribution patterns. For climate trend analysis, ERA5-Land hourly datasets (1950–2021) of temperature and precipitation at 9 km resolution were processed. Trend detection was conducted using the Modified Mann-Kendall test and Thiel-Sen's slope estimator across five overlapping 30-year climatic windows (1951–1980, 1961-1990, ... 1991–2020) and the full 72-year period (1950-2021), with anomalies calculated relative to the 1961–1990 baseline per WMO guidelines. Positive Degree Days (PDD $> 0°C$) were computed as a melt indicator, with their spatiotemporal trends analyzed to quantify warming impacts on cryospheric processes. The comprehensive methodology integrated satellite-derived snow cover patterns with long-term climate trends, enabling robust assessment of snow cover-climate interactions while accounting for

topographic controls. All statistical analyses were performed at 5% significance level using established computational frameworks, ensuring methodological rigor in detecting climate-driven changes in the ZRB's cryosphere. The overlapping multiple climate window approach facilitated identification of both gradual trends and abrupt shifts in snow cover dynamics under changing climatic conditions.

5.2 Conclusions

Based on the analysis carried out following specific conclusion were derived,

5.2.1 Snow cover distribution patterns

The spatial distribution of snow cover in the ZRB demonstrates clear elevational dependence, with elevation emerging as the primary driver of snow persistence. Critical thresholds are observed near the 4,000-5,000 m elevation band, where snow cover transitions from seasonal to near-perennial conditions. Slope angle and aspect further modulate snow retention patterns through their influence on insolation and terrain-driven microclimates. Notably, steep north-facing slopes function as important climate refugia for snow preservation due to reduced solar exposure. Across all aspects, solar radiation emerges as the dominant control on snow cover variability, with southern aspects particularly prone to accelerated melt rates due to prolonged direct sunlight exposure. These topographic controls collectively shape the basin's heterogeneous snow cover distribution and its vulnerability to climate warming. Salients points are as follows:

1. Strong altitudinal control exists, with near-perennial snow cover (>77% mean) above 5,000 m and high variability (0.2–95.8%) below 4,000 m, reflecting elevation-dependent warming effects.

2. The 4,000–5,000 m transitional zone shows moderate snow persistence (55.9%

mean), indicating thresholds where seasonal melt dominates but snow accumulation remains significant.

3. Optimal snow retention occurs on 20–50° slopes (60–64% mean), balancing gravitational shedding and insolation, while >50° slopes paradoxically retain the most snow (68.6% mean), likely due to shading or wind-driven deposition.

4. Gentle slopes (0–10°) exhibit lower snow persistence (54.7% mean), attributed to enhanced melt from solar exposure and debris/vegetation cover.

5. North-facing slopes retain the most snow (68.2% mean) due to minimal solar radiation, while south-facing slopes show the least persistence (58.5% mean) from prolonged insolation.

6. East-facing slopes (66.1% mean) retain more snow than west-facing (62.2% mean), likely due to cooler morning melt conditions compared to warmer afternoon exposure.

5.2.2 Temporal pattern of snow cover extent

The analysis of MODIS snow cover data (2000-2020) revealed distinct seasonal patterns, with maximum coverage occurring in winter/early spring (Jan-Apr, peaking at 91-95%) and minimum coverage in late summer (Aug, 24%). Interannually, snow cover averaged 64%, ranging from 55% (2011-2012) to 74% (2009-2010). The period Mar-May showed consistently high snow cover (>75%) across most years, serving as a critical storage phase before melt onset. Notable variability was observed in transitional months, particularly June (37-77% coverage), reflecting temperature sensitivity. Exceptionally high snow years (e.g., 2009-2010) featured near-complete winter coverage, while low years (e.g., 2011-2012) indicated reduced accumulation. Some years (e.g., 2016-2017) exhibited delayed but intense snowfall events, compensating for late-season accumulation. The findings highlight both the robust seasonality of ZRB's snow cover and its vulnerability to interannual climate fluctuations, with implications for regional hydrology and water resource management. Analysis was restricted to <15% cloud cover days to ensure data

reliability. The trend analysis of snowfall revealed meaningful insights as listed below,

1. The post-2000 period (2001–2020) exhibited a marked increase in the frequency and severity of negative snowfall anomalies compared to previous decades. Annual snowfall deficits occurred in 70% of years (vs. 40-60% pre-2000), with extreme deficits (e.g., -206.6 mm w.e. in 2016). Winter and summer snowfall also showed higher deficits, suggesting a climatic shift toward reduced snow accumulation.

2. Winter snowfall anomalies, critical for water storage, displayed persistent negative trends post-2000 (50% of years), with severe deficits (e.g., -172.1 mm w.e. in 2017). While frequency matched some earlier periods, the magnitude and clustering of deficits imply potential weakening of westerly disturbances or warming-induced snowpack decline.

3. Summer snowfall anomalies shifted dramatically post-2000, with 85% of years showing negative deviations (vs. 55-65% pre-2000) and record deficits (e.g., -84.6 mm w.e. in 2016). This trend aligns with rising temperatures or altered monsoon dynamics, reducing summer snow contribution to hydrology.

4. The ZRB exhibited a long-term (1950-2020) decline in annual snowfall, though trends were statistically insignificant, suggesting natural variability dominates. Early periods (1951–1980) mirrored this decline, while 1961–1990 saw localized increases (significant in southwestern/northeastern areas). Recent windows (1981–2010, 1991–2020) show spatially extensive but statistically insignificant negative trends, hinting at potential early-stage declines linked to warming.

5. Early periods (1951-1980, 1961-1990) featured nonsignificant trends, while 1991–2020 revealed coherent negative trends, including statistically significant declines in some of the grid cells. This signals accelerating summer snowfall loss, likely tied to rising temperatures.

6. The 1961-1990 window stood out with basin-wide significant positive trends, but subsequent periods (1971-2000 onward) reverted to statistically non-significant declines, particularly in the southeast part of the region (1981–2010). This seasonal divergence underscores winter's resilience compared to summer but highlights recent weakening accumulation.

7. The basin-wide analysis revealed predominantly negative (though statistically non-significant) trends in annual snowfall, suggesting a gradual decline in total accumulation. The 5-year moving window approach confirmed this pattern, with winter increases partially offsetting summer losses but insufficient to reverse the overall negative trajectory. This implies that while annual snowfall reductions remain within natural variability, their persistence across decades aligns with broader warming trends.

8. Summer snowfall exhibited robust, statistically significant declines across most of the basin, underscoring its heightened sensitivity to climate change. The consistent negative trends found in 5-year moving windows—particularly the significant long-term reduction (1950-2020). Given summer's contribution to seasonal snowpack, these declines carry critical implications for water availability and glacier mass balance.

9. Winter trends contrasted sharply with summer patterns, showing predominantly positive (but non-significant) accumulation changes. The lack of statistical significance suggests these increases may reflect natural variability rather than a climatic signal. However, their persistence raises questions about potential elevation-dependent warming effects or shifts in winter storm tracks, warranting further investigation into seasonal atmospheric drivers.

5.2.3 Temporal pattern of temperature

Analysis of ERA5-Land temperature data (2000-2020) for the ZRB reveals strong seasonality, with winter (Dec-Feb) averaging -20.6°C (coldest in January: -23.0°C)

and summer (Jun-Aug) reaching 4.9-5.2°C. Spring (Mar-May) shows gradual warming (-17.4°C in March to -7.0°C in May), delayed by snow-cover feedbacks, while autumn (Oct-Nov) features rapid cooling (-7.5°C to -14.7°C). Interannual variability includes extremes like October 2018 (-14.5°C) and September 2018 (+2.3°C). The basin's cryospheric dominance is evident, with 8 months below freezing and an annual mean of -9.5°C. The extended sub-zero period (Oct-May) sustains snowpack, while the brief ablation window (Jun-Sep) controls meltwater release. Transitional months (Apr, Oct) exhibit high variability, potentially shifting melt onset and accumulation timing. These findings highlight the ZRB's sensitivity to climate change, with implications for glacier dynamics and water resources. The salient findings from the anomaly and trend analysis are as follows,

1. The ZRB has experienced a dramatic warming shift post-2000, with 85% of years showing positive temperature anomalies (relative to 1961-1990) and a 0.56°C increase in mean annual anomalies (+0.57°C in 2001-2020 vs. -0.01°C in 1950-2000). Unprecedented multiyear warm sequences (e.g., 2001-2008) and record anomalies nearing +2.0°C (2007, 2016) highlight a ongoing climatic regime shift.

2. The ZRB exhibited statistically significant warming across all grid points, with annual and summer mean temperatures showing consistent increases, indicating a clear regional response to climate change.

3. The trend analysis of annual average mean temperature in multiple overlapping climate window reveals distinct phases—early warming (1951-1980), mixed/cooling trends (1961-1990, 1971-2000), and accelerated warming (1981-2010 onward). Notably, the 1991-2020 window reversed earlier spatial patterns, with significant warming in most areas but non-significant cooling in the southwest.

4. Summer trends mirrored annual patterns but with stronger recent warming (1991-2020), in comparison to annual average mean temperature. This underscores the basin's vulnerability to seasonal amplification of warming.

5. The trend analysis in 5 year moving window reveals statistically significant

warming across all grid points for both annual and summer mean temperatures (5% significance level), demonstrating a systematic and spatially extensive climatic shift. Post-2000, PDD anomalies surged to +6 PDD (vs. -0.95 PDD in 1951–1970), with record-breaking warm extremes (e.g., +29 PDD in 2000) becoming frequent, while cold anomalies diminished—indicating accelerated thermal forcing with critical implications for glacier melt and hydrological regimes.

6. While 1951–2000 exhibited variable PDD trends (mostly non-significant within the basin), a clear transition occurred post-1980, with 1981–2010 and 1991–2020 windows showing statistically significant PDD increases in some of the regions.

5.3 Challenges and limitations of the study

The study relies on MODIS MOD10A2 8-day composite data (500 m resolution), which, while providing readily available snow cover extent, lacks the finer spatial detail offered by other higher-resolution satellites (e.g., Sentinel, Landsat, or Resourcesat). The coarse resolution limits fine-scale snow cover analysis, potentially obscuring small-scale variability in snow distribution, particularly in complex mountainous terrain. Although higher-resolution datasets (e.g., Sentinel-2 at 10–20 m, Landsat8 30 m) could improve accuracy, their lack of pre-processed snow cover products increases processing complexity, making MODIS a pragmatic but constrained choice.

The absence of long-term in-situ observations in the high-altitude ZRB necessitated the use of ERA5-Land reanalysis data for temperature and snowfall analysis. While ERA5-Land is widely used in data-scarce regions, its performance in accurately resolving snowfall and temperature extremes in high-altitude zones remains unvalidated for the ZRB. Potential uncertainties arise from model biases, topographic smoothing (9 km resolution), and parameterization schemes, which may not fully capture local microclimatic conditions.

These limitations highlight trade-offs between data availability and resolution, emphasizing the need for future validation efforts and integration of higher-resolution datasets where feasible.

5.4 Contributions and recommendations for future work

The research conducted in this study holds significant practical and scientific relevance. Its findings are expected to provide valuable insights for hydrologists, particularly in the analysis of water resources and the response of river basins to climate change in North-Western Himalayas. This study makes three key contributions:

1. The study provides the first comprehensive assessment of snow cover distribution in the ZRB, identifying critical elevation thresholds (4,000–5,000 m) where snow transitions from seasonal to near-perennial.

2. It documents a post-2000 climatic shift in ZRB, with 70% and 85% of years showing annual and summer snowfall deficits, respectively and 80% of year exhibiting positive temperature anomalies with respect to the baseline period.

3. It confirms accelerated warming in 1991–2020 in ZRB, particularly in summer, with record PDD anomalies (e.g., +29 PDD in 2000) driving enhanced melt.

The limitations and challenges encountered in this research present opportunities for refining the results and gaining deeper insights into the findings. The following four recommendations are proposed for future research endeavors to address these challenges and enhance the robustness of the analysis:

5.4. Contributions and recommendations for future work

1. Integration Sentinel-2/Landsat data (10–30 m) to resolve fine-scale snow dynamics, particularly in transitional elevation zones (4,000–5,000 m).
2. Establishment of high-altitude weather stations to validate ERA5-Land snowfall and temperature estimates, addressing reanalysis uncertainties.
3. Investigation of elevation-dependent warming mechanisms using downscaled climate models.
4. Analysis of atmospheric drivers(e.g., westerly disturbances, monsoon shifts) behind snowfall variability.

References

Aggarwal, S., Thakur, P. K., Nikam, B. R., & Garg, V. (2014). Integrated approach for snowmelt run-off estimation using temperature index model, remote sensing and gis. *Current Science*, *106*(3), 397–407.

Ali, S. N., Agrawal, S., Sharma, A., Phartiyal, B., Morthekai, P., Govil, P., Bhushan, R., Farooqui, S., Jena, P. S., & Shivam, A. (2020). Holocene hydroclimatic variability in the zanskar valley, northwestern himalaya, india. *Quaternary Research*, *97*, 140–156.

Bisht, D. S., Chatterjee, C., Raghuwanshi, N. S., & Sridhar, V. (2018). An analysis of precipitation climatology over indian urban agglomeration. *Theoretical and Applied Climatology*, *133*, 421–436.

Chahal, P., Kumar, A., Sharma, C. P., Singhal, S., Sundriyal, Y., & Srivastava, P. (2019). Late pleistocene history of aggradation and incision, provenance and channel connectivity of the zanskar river, nw himalaya. *Global and Planetary Change*, *178*, 110–128.

Dharpure, J. K., Patel, A., Goswami, A., Kulkarni, A. V., & Snehmani (2020). Spatiotemporal snow cover characterization and its linkage with climate change over the chenab river basin, western himalayas. *GIScience & Remote Sensing*, *57*(7), 882–906.

Hall, D. K., Riggs, G. A., & Salomonson, V. V. (1995). Development of methods for mapping global snow cover using moderate resolution imaging spectroradiometer data. *Remote sensing of Environment*, *54*(2), 127–140.

Hall, D. K., Riggs, G. A., Salomonson, V. V., Barton, J., Casey, K., Chien, J., DiGirolamo, N., Klein, A., Powell, H., & Tait, A. (2001). Algorithm theoretical basis document (atbd) for the modis snow and sea ice-mapping algorithms. *Nasa Gsfc*, *45*, 14–28.

Hussain, M., & Mahmud, I. (2019). pymannkendall: a python package for non parametric mann kendall family of trend tests. *Journal of open source software*, *4*(39), 1556.

Jain, S. K., Goswami, A., & Saraf, A. K. (2008). Accuracy assessment of modis, noaa and irs data in snow cover mapping under himalayan conditions. *International Journal of Remote Sensing*, *29*(20), 5863–5878.

Maurer, J. M., Schaefer, J., Rupper, S., & Corley, A. (2019). Acceleration of ice loss across the himalayas over the past 40 years. *Science advances*, *5*(6), eaav7266.

Sharma, A., & Phartiyal, B. (2020). Geomorphological changes during quaternary period vis a vis role of climate and tectonics in ladakh, trans-himalaya. *Himalayan Weather and Climate and their Impact on the Environment*, (pp. 159–183).

Shukla, S., Kansal, M. L., & Jain, S. K. (2017). Snow cover area variability assessment in the upper part of the satluj river basin in india. *Geocarto International*, *32*(11), 1285–1306.

Snehmani, Dharpure, J. K., Kochhar, I., Hari Ram, R., & Ganju, A. (2016). Analysis of snow cover and climatic variability in bhaga basin located in western himalaya. *Geocarto International*, *31*(10), 1094–1107.

Taylor, P. J., & Mitchell, W. A. (2000). The quaternary glacial history of the zanskar range, north-west indian himalaya. *Quaternary International*, *65*, 81–99.

WMO (2017). Wmo guidelines on the calculation of climate normals. *World Meteorological Organization. Geneva.*